Soil Use and Management

WILEY | BRITISH SOCIETY OF SOIL SCIENCE

RESEARCH ARTICLE OPEN ACCESS

Carbon Input and Tillage Intensity Modulate Pedo-Climatic Controls of Topsoil but Not Subsoil Physical Properties

Olivier Heller[1] | Tommy D'Hose[2] | Pia Euteneuer[3] | Miroslav Fér[4] | Marta Goberna[5] | Nicholas Jarvis[6] | Lars J. Munkholm[7] | Elsa M. Arrázola-Vásquez[6] | Luca Bragazza[8] | Shiva Ghiasi[1] | Thomas Guilaume[8] | Marcel G. A. van der Heijden[1,9] | John Koestel[1] | Anna Lindahl[6] | Jochen Mayer[1] | Markéta Mayerová[10] | Johannes W. M. Pullens[7] | Bano Mehdi-Schulz[11] | Inés Santín[5] | Lorena Chagas Torres[6] | Raphaël Wittwer[1] | Thomas Keller[1,6] | Loraine ten Damme[7]

[1]Division of Agroecology and Environment, Agroscope, Zürich, Switzerland | [2]Flanders Research Institute for Agriculture, Fisheries and Food (ILVO), Merelbeke-Melle, Belgium | [3]Department of Agricultural Sciences, Experimental Farm Gross-Enzersdorf, BOKU University, Groß-Enzersdorf, Austria | [4]Faculty of Agrobiology Food and Natural Resources, Department of Soil Science and Soil Protection, Czech University of Life Sciences Prague (CZU), Prague, Czech Republic | [5]Department of Environment and Agronomy, Instituto Nacional de Investigación y Tecnología Agraria y Alimentaria, Spanish National Research Council (INIA, CSIC), Madrid, Spain | [6]Department of Soil and Environment, Swedish University of Agricultural Sciences (SLU), Uppsala, Sweden | [7]Department of Agroecology, Aarhus University, Foulum, Denmark | [8]Field-Crop Systems and Plant Nutrition, Agroscope, Nyon, Switzerland | [9]Department of Evolutionary Biology and Environmental Studies, University of Zürich, Zürich, Switzerland | [10]Czech Agrifood Research Center, Prague, Czech Republic | [11]Department of Landscape, Water and Infrastructure, Institute of Hydrology and Water Management, BOKU University, Vienna, Austria

Correspondence: Olivier Heller (olivier.heller@agroscope.admin.ch)

Received: 27 November 2025 | **Revised:** 27 May 2026 | **Accepted:** 4 June 2026

Keywords: long-term field experiments | soil functions | soil health | soil quality | structural equation modelling

ABSTRACT

Soil functions such as water regulation, resistance to degradation (i.e., erosion) and habitat provision for soil biota are essential for climate-resilient cropping systems. While soil functions are largely governed by pedo-climatic conditions, the relative importance of agricultural management remains unclear. Because these functions are governed by soil physical properties, we quantified the relative influence of pedo-climatic conditions and soil management on key soil physical properties across ten long-term field experiments in Europe. The sites spanned a 2500 km climatic gradient from Spain to Sweden and included contrasting tillage or organic matter management practices. Measurements included bulk density (BD), water storage, aeration, hydraulic conductivity, soil organic carbon (SOC), aggregate stability, and earthworm abundance in topsoil (~10 cm) and subsoil (~30 cm) across 92 plots and 23 management treatments. Management intensities (carbon inputs, tillage, mineral nitrogen fertilisation) were quantified over the preceding decade. We applied mixed-effects models, variance partitioning and structural equation modelling to identify direct and indirect effects. Pedo-climatic conditions explained more variability in soil physical properties than management (threefold in the topsoil and eightfold in the subsoil). Mean annual temperature and clay content controlled topsoil SOC content, which in turn mediated most soil physical properties. Management effects, although smaller, significantly influenced topsoil properties. Higher C inputs increased SOC, aggregate stability and earthworm abundance. These effects indirectly reduced BD and penetration resistance while increasing water storage, air capacity and hydraulic conductivity. Higher tillage intensity reduced BD directly but was also associated with lower aggregate stability and reduced saturated hydraulic conductivity in the topsoil. Overall, pedo-climatic conditions dominated soil physical properties, particularly in the subsoil, whereas management mainly affected topsoil properties relevant for climate resilience, highlighting limited subsoil responsiveness and the need for management strategies targeting subsoils.

Thomas Keller and Loraine ten Damme have contributed equally to this work.

1 | Introduction

Soil structure related functions such as water regulation, resistance to degradation (i.e., erosion) and habitat provision for soil biota are central to sustaining agricultural production and buffering crop yields against climate extremes (Rabot et al. 2018; Saco et al. 2021). By regulating plant-available water and crop rooting conditions, soil physical properties directly affect the climate resilience of cropping systems (Bodner et al. 2015). Maintaining or improving these properties through adapted soil management is therefore an important long-term objective in arable farming (Heitman et al. 2023).

Soil management practices, such as tillage, organic matter amendments, crop rotation and cover cropping, are known to influence soil physical properties (e.g., Strudley et al. 2008; Blanco-Canqui and Ruis 2018; Palm et al. 2014; Basset et al. 2023). A recent synthesis of 34 meta-analyses confirmed that organic amendments and systems with continuous soil cover improve the water regulation function, whereas the effects of reduced tillage remain context-dependent (Blanchy, Bragato, et al. 2023). However, the magnitude of management effects varies widely and is often constrained by site-specific factors such as soil texture and climate (Sun et al. 2020; Blanchy, Albrecht, et al. 2023).

The literature synthesis of Sánchez-Moreno et al. (2025) found varying effects of management-induced increases in soil organic matter on topsoil physical properties across sites. In contrast, data for subsoils remain scarce (Sánchez-Moreno et al. 2025; Yost and Hartemink 2020), but the few conducted studies have reported no significant management effects on subsoil structure (e.g., Schlüter et al. 2011; Jarvis et al. 2017). This raises the questions of how strongly management can modify soil properties relative to pedo-climatic constraints, under which environmental conditions management can effectively improve soil properties, and whether these effects are restricted to the topsoil or extend into the subsoil. Long-term field experiments (LTEs) offer an opportunity to address this question, as they provide decades of consistent management treatments under well-documented site conditions. Yet, systematic cross-site comparative studies using harmonised data collection and integrated data analysis across large pedo-climatic gradients remain rare, particularly for subsoil properties.

In this study, we investigated ten LTEs across Europe to assess how tillage practices and organic matter management influence soil properties. Using a harmonised sampling protocol and statistical modelling, we disentangled the relative influence of management and pedo-climatic context on key hydraulic and mechanical properties in topsoil and subsoil layers. Specifically, we quantified the effects of tillage intensity (STIR), carbon inputs (C inputs), mineral nitrogen fertilisation (N_{min} input), soil texture and climate (precipitation and temperature) on soil organic carbon (SOC) content, bulk density (BD) and earthworm abundance, and evaluated how these moderators of soil structure influence soil properties related to water regulation, erosion control and soil aeration (Figure 1). We further assessed the relative importance of management and pedo-climatic condition in shaping topsoil and subsoil physical properties. To this end, we addressed the following research questions: (1) How do management practices influence SOC, BD and earthworm abundance? (2) To what extent do these variables mediate management effects on other soil physical properties? (3) What is the relative importance of pedo-climatic conditions, represented by soil texture and climate, in explaining variation in soil physical properties, particularly in the subsoil?

2 | Methods

2.1 | Long-Term Experiments: Soil Management Indicators and Site Characteristics

This study included 111 plots in ten long-term field experiments (LTEs) in different pedo-climatic contexts (Table 1). For each LTE, two to four treatments with contrasting soil management were selected. The treatments either differed in tillage practices (inversion tillage, reduced tillage and no tillage), organic matter management (organic amendments and crop residue retention)

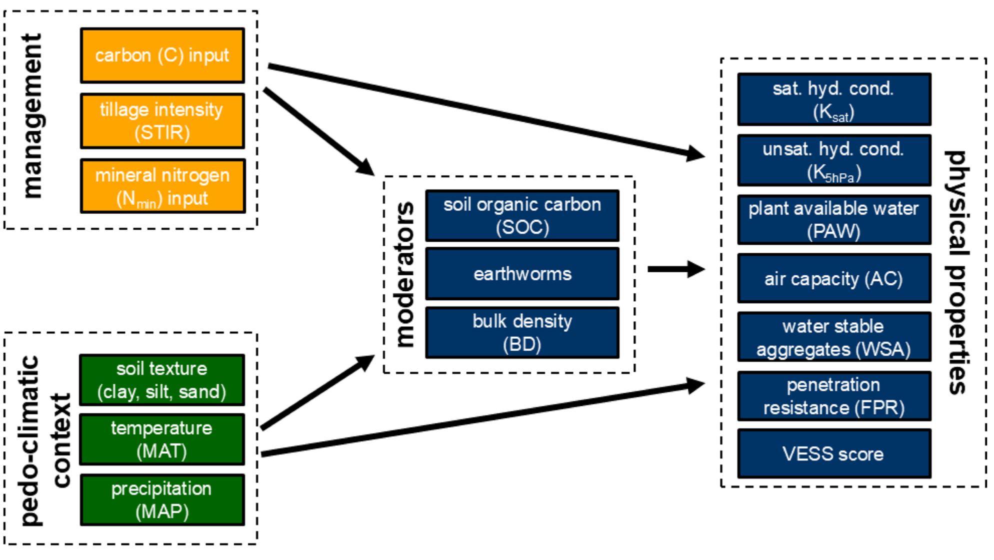

FIGURE 1 | Conceptual figure illustrating how soil management and site-inherent pedo-climatic context are assumed to directly and indirectly affect soil physical properties. Indirect effects of soil management and pedo-climatic context on the physical properties were assumed to be mediated by the moderators (earthworm abundance, SOC, BD).

TABLE 1 | Description of the 10 long-term field experiments (LTE).

Experiment (source)	Place (coordinates, elevation)	Soil type/Soil texture[a]/MAP[b]/MAT[c]	Since/blocks/plot size	Crop rotation	Treatment	Description[d]
BOPA (D'Hose et al. 2016)	Merelbeke, Belgium (50.9855°, 3.7738°, 21 m a.s.l)	Bathygleyic Cambisol/Sandy Loam/720 mm/11.2°C	2010/4 blocks/225 m^2	Silage maize[e] Potato[e] Spring barley[e] Leek[e] or Fodder beet[e]	ITC	Inversion tillage (30 cm), compost, cattle slurry and mineral fertilisation
					ITP	Inversion tillage (30 cm), pig slurry and mineral fertilisation
					RTC	Reduced tillage (Subsoiler, 30 cm; Seedbed preparation), compost, cattle slurry and mineral fertilisation
					RTP	Reduced tillage (Subsoiler, 30 cm; Seedbed preparation), pig slurry and mineral fertilisation
CASL (Hlisnikovský et al. 2020)	Čáslav, Czech Republic (49.8913°, 15.3945°, 267 m a.s.l)	Greyzemic Phaeozem/Silt Loam/555 mm/9.0°C	1955/4 blocks/64 m^2	Winter wheat Silage maize Winter rapeseed Winter wheat Potato Spring barley Red clover	FYM	Inversion tillage (24 cm), farmyard manure
					MIN	Inversion tillage (24 cm), no fertilisation
CENT (Gómez-Muñoz et al. 2021)	Flakkebjerg, Denmark (55.3279°, 11.3820°, 30 m a.s.l)	Glossic Phaeozem/Sandy Loam/494 mm/9.2°C	2002/4 blocks/36 m^2	Winter wheat[e] Spring barley[e] Spring oats[e] Faba bean Winter wheat[e] Spring barley[e] Spring oats	ITR	Inversion tillage (20 cm), residue removal
					ITS[f]	Inversion tillage (20 cm), residue retention
					NTR[f]	No-till, residue removal
					NTS	No-till, residue retention
FAST (Wittwer et al. 2021)	Rümlang, Switzerland (47.4389°, 8.5278°, 443 m a.s.l.)	Calceric Cambisol/Loam/1002 mm/10.2°C	2009/4 blocks/45 m^2	Grain maize Spring pea[e] Winter wheat Temporary ley (2 years) Winter wheat[e]	CIT	Inversion tillage (20 cm), mineral fertilisation
					CNT	No-till farming system, mineral fertilisation.
					OIT[f]	Organic farming system, inversion tillage (20 cm), organic fertilisation with cattle slurry
					ORT[f]	Organic farming system, reduced tillage (Chisel, < 10 cm; Seedbed preparation), organic fertilisation with cattle slurry

(Continues)

TABLE 1 | (Continued)

Experiment (source)	Place (coordinates, elevation)	Soil type/ Soil texture[a]/ MAP[b]/MAT[c]	Since/blocks/ plot size	Crop rotation	Treatment	Description[d]
HOLL (Rosner et al. 2018)	Hollabrunn, Austria (48.5627°, 16.0649°, 239 m a.s.l.)	Chernozem/Silt Loam/478 mm/10.4°C	2009/3 blocks/300 m^2	Winter wheat[e] Sunflower Spring pea Winter wheat[e] Grain maize Winter wheat[e] Spring barley[e] Soybean Winter wheat	ITS	Inversion tillage (25 cm), residue retention, mineral fertilisation
					NTS	No-till, residue retention, mineral fertilisation
INIA (Martin-Rueda et al. 2007)	Madrid, Spain (40.5159°, −3.3101°, 599 m a.s.l.)	Calcic Cambisol/ Loam/361 mm/14.7°C	1994/4 blocks/250 m^2	Winter wheat Winter wheat or vetch Winter wheat or barley Winter wheat or fallow	ITM	Inversion tillage (25 cm), wheat monoculture, mineral fertilisation
					ITR	Inversion tillage (25 cm), crop rotation, mineral fertilisation
					NTM	No-till, wheat monoculture, mineral fertilisation
					NTR	No-till, crop rotation, mineral fertilisation
LUKA (Hlisnikovský et al. 2020)	Lukavec, Czech Republic (49.5566°, 14.9783°, 628 m a.s.l.)	Eutric Cambisol/Sandy Loam/580 mm/8.7°C	1955/4 blocks/64 m^2	Winter wheat Silage maize Winter rapeseed Winter wheat Potato Spring barley Red clover	FYM	Inversion tillage (20 cm), farmyard manure
					MIN	Inversion tillage (20 cm), no fertilisation
P24A (Maltas et al. 2018)	Nyon, Switzerland (46.4004°, 6.2295°, 446 m a.s.l.)	Calcaric Cambisol/ Loam/1084 mm/10.8°C	1976/4 blocks/90 m^2	Grain maize Winter wheat Spring barley Winter rapeseed Spring oat Winter wheat	MIN	Inversion tillage (22 cm), mineral fertilisation
					FYM	Inversion tillage (22 cm), farmyard manure, mineral fertilisation

(Continues)

TABLE 1 | (Continued)

Experiment (source)	Place (coordinates, elevation)	Soil type/Soil texture[a]/MAP[b]/MAT[c]	Since/blocks/plot size	Crop rotation	Treatment	Description[d]
SAEB (Torppa and Taylor 2022)	Uppsala, Sweden (59.8325°, 17.7054°, 11 m a.s.l.)	Eutric Cambisol/Loam/487 mm/6.9°C	2006/3 blocks/180 m^2	Winter wheat Winter wheat Spring barley or w. rapeseed Spring wheat Spring barley or spring peas	ITC	Inversion tillage (23 cm), cereal rotation, mineral fertilisation
					ITD	Inversion tillage (23 cm), diverse rotation, mineral fertilisation
					NTD[f]	No-till, diverse rotation, mineral fertilisation
ZOFE (Oberholzer et al. 2014)	Zürich, Switzerland (47.4268°, 8.5188°, 438 m a.s.l.)	Haplic Luvisol/Sandy Loam/1001 mm/10.2°C	1949/4 blocks/35 m^2	Grain maize Winter wheat[e] Spring wheat[e] Spring barley Temporary ley (2 years) Winter wheat[e] Grain maize Potato Winter wheat[e]	MIN	Inversion tillage (18 cm), mineral fertilisation (with mineral nitrogen)
					COM	Inversion tillage (18 cm), compost, mineral fertilisation (without mineral nitrogen)

[a]According to USDA textural classes (Soil Science Division Staff 2017).
[b]Mean annual precipitation 1991–2020 (data exctracted from Agri4Cast (JRC, n.d.)).
[c]Mean annual temperature 1991–2020 (same source as MAP).
[d]Includes the maximum depth of tillage operations and details on the reduced tillage technique; inversion tillage always includes ploughing and seedbed preparation.
[e]Crop followed by a cover crop.
[f]This treatment was excluded from the current study due to missing data for at least one soil property; all available data are obtainable online (Heller, ten Damme, et al. 2024).

or both. Within the LTEs, each treatment was spatially replicated three or four times (Table 1).

To quantify soil management intensity variations within and across LTEs, we calculated soil management indicators for each plot with the software package *SoilManageR* for R (Heller et al. 2025). Specifically, average annual C input by crops, cover crops and organic amendments (Mg C $ha^{-1}year^{-1}$), average yearly STIR ($year^{-1}$), and average annual N_{min} input by mineral fertilisers (kg N $ha^{-1}year^{-1}$) were calculated based on information on management operations, crop yield and organic amendments for the ten years prior to sampling. A detailed description of how *SoilManageR* derives soil management indicators is published in Heller et al. (2025), and the calculated management indicators for our ten LTEs are shown in Figure 2a. In brief, the C input ranged from 1.0 to 7.9 Mg C $ha^{-1}year^{-1}$, with a majority of the treatments between 1.7 and 4.5 Mg C $ha^{-1}year^{-1}$. The lowest C inputs occurred in the unfertilised treatments at LUKA and CASL (both in Czech Republic), and the treatments with temporary fallow at INIA (Spain). The highest C inputs occurred in the treatments that received cattle slurry and compost at BOPA (Belgium). STIR values were between 1 and 228, with the lowest annual STIR values calculated for the no tillage treatments at CENT (Denmark), FAST (Switzerland), HOLL (Austria) and INIA (Spain). The BOPA trial had the highest STIR value of 288 $year^{-1}$ due to annual double tillage—once for main crops and once for cover crops—as well as additional tillage operations to incorporate solid organic amendments. N_{min} input ranged between 0 and 128 kg N $ha^{-1}year^{-1}$ with a majority of treatments between 57 and 101 kg N $ha^{-1}year^{-1}$.

Mean annual precipitation sum (MAP; average of years 1991–2020) at the LTE sites ranged from 361 to 1084 mm (Figure 2b), and mean annual temperatures (MAT; average of years 1991–2020) were between 6.9°C and 14.7°C. Management intensity indicators and climatic descriptors were uncorrelated (all $|r| < 0.5$, data not shown). Soil types at the LTEs included seven soils from the Cambisol–Luvisol chronosequence, two Phaeozems (CENT and CASL) and one Chernozem (HOLL). Soil textures at the LTE sites were loamy, with texture classes ranging from silt loams to sandy loams (Figure 2c). Consequently, there was a strong negative correlation between silt and sand in the dataset (Pearson's correlation coefficient $r = -0.93$, p-value < 0.001, Figure S1) and we therefore excluded silt as an explanatory variable for this study.

2.2 | Soil Sampling and Assessment

Soil physical properties were measured in the ten LTEs, together with chemical and biological properties hypothesised to influence them. A comprehensive protocol was developed to harmonise the sampling and analysis among the LTEs (Heller, D'Hose, et al. 2024). A report on the sampling and measurement campaign is available online (Holzkämper et al. 2024) and is only briefly summarised here.

Three undisturbed soil cores were collected at randomly selected positions within each plot, avoiding plot edges, with core centres at 10 and 30 cm depth representing the topsoil and subsoil, respectively. These depths were chosen to sample soil within and below the plough layer of the ploughed treatments while maintaining comparability across sites. In the BOPA trial, sampling depths were adjusted to 5 cm for the topsoil and 45 cm for the subsoil to match the local tillage depth of 30 cm (Table 1). In this trial, only one soil core was taken per plot and depth. No depth correction was applied in the statistical analysis. The volume of the soil cores was 100 cm^3 for the LTEs in Spain, Denmark and Czech Republic (CASL, CENT, INIA, LUKA) as well as for the subsoils of two Swiss LTEs (P24A and ZOFE), and 250 cm^3 for the remaining LTEs and depths.

Representative composite soil samples of at least 500 g were prepared from five subsamples per plot and depth, and used for

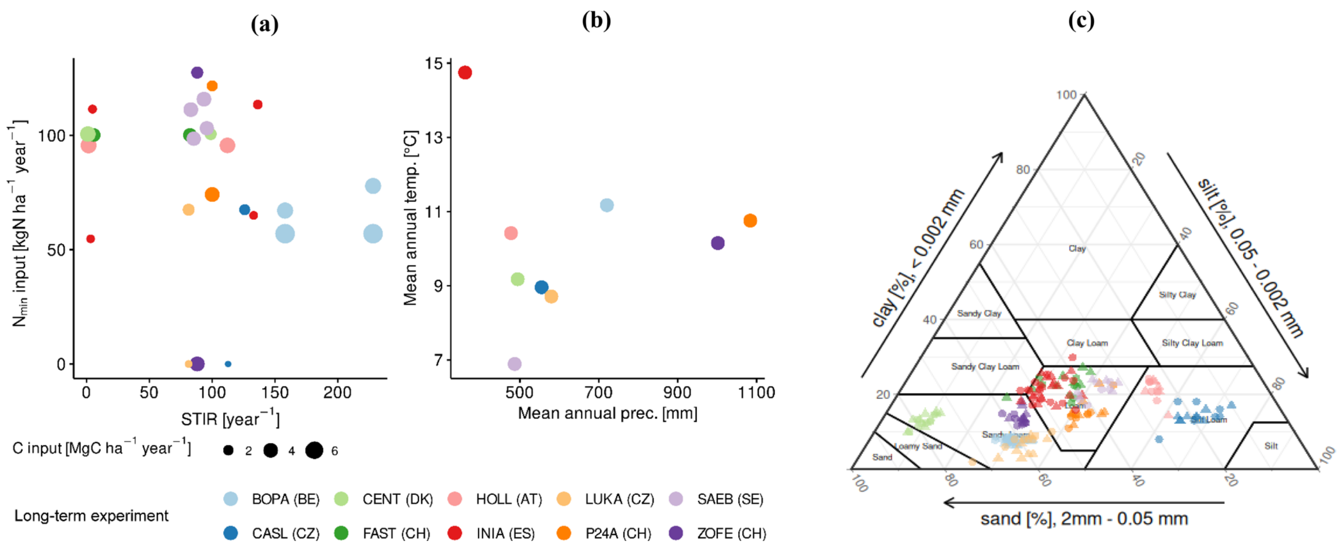

FIGURE 2 | Soil texture, management indicators and climatic descriptors. (a) soil textural triangle with all soil samples in the data set. Circles indicate measurements from the topsoil (10 cm) and triangles measurements from the subsoil (30 cm). In the numerical soil management indicators (b) and climatic descriptors (c) the colours indicate the long-term field experiment. Details of the long-term experiment (incl. abbreviations) can be found in Table 1. Climatic descriptors for the period between 1991 and 2020 were extracted from the European crop forecasting and monitoring system Agri4Cast (JRC, n.d.).

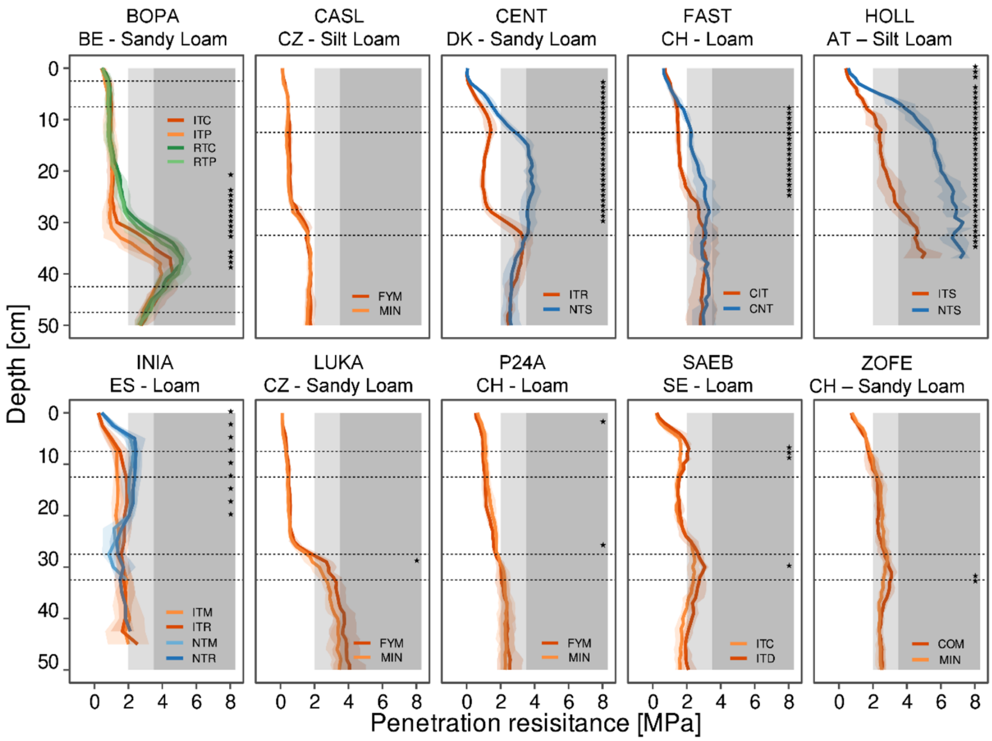

FIGURE 3 | Mean soil penetration resistance (FPR) of each treatment in the ten long term field experiments. Colour codes refer to treatments, the coloured shades represent the standard deviation within each treatment. Star symbols (★) mark depths where the penetration resistance differs significantly between treatments (p-value <0.05). Abbreviations for long-term experiments and treatments can be found in Table 1. The dashed horizontal lines represent the upper and the lower boundary of the sampling depth for the topsoil and the subsoil, respectively. The grey areas indicate penetration resistances that are considered to restrict root growth: >2 MPa (light grey, Bengough et al. 2011) and >3.5 MPa (dark grey; Moraes et al. 2014).

measurements of soil texture (clay, silt, sand), particle density (PD), SOC content and water stable aggregates index (WSA). Field penetration resistance (FPR, Figure 3) was measured to a depth of at least 40 cm using penetrologgers (Penetrologger PRO, Royal Ejkelkamp, The Netherlands; FieldScout SC 900, Spectrum Technologies Inc., USA) or a custom-built device as described in Olsen (1988) with the median value recorded from at least 10 insertions per plot. The average FPR of the depths where intact soil cores were taken (i.e., 10 and 30 cm; 5 and 45 cm for BOPA) was extracted to compare the FPR to the soil core-derived soil physical properties. Earthworm abundance was quantified through a meticulous manual sorting of soil blocks (20 cm × 20 cm × 20 cm). The manual sorting was complemented by using 500 mL mustard solution expulsion per pit (5 g mustard powder L^{-1}; Butt and Grigoropoulou 2010), except in the Danish and Spanish LTEs (CENT and INIA) where applying mustard solution was not allowed. Topsoil structure was evaluated using the Visual Evaluation of Soil Structure (VESS) method (Guimarães et al. 2011, 2017). The number of earthworm observations and VESS scores recorded per plot ranged from one to four.

All sampling was conducted in spring 2023 before spring tillage operations, with the exception of INIA, where the sampling was postponed to Autumn 2023 due to unusual dry conditions in spring. For SAEB (Sweden) and BOPA, earthworm sampling was conducted in September and November of 2024, respectively.

On a total of 757 soil cores (111 plots, 2 to 3 depths, 1 to 4 soil cores per plot) saturated and near-saturation hydraulic conductivity (K_{sat} and K_{5hPa}) were measured using mini disk infiltrometers (Meter Group GmbH, Germany; Sarkar et al. 2019a, 2019b). K_{5hPa} is considered here to represent the saturated hydraulic conductivity of the soil matrix, whereas K_{sat} additionally includes the contribution of all large macropores with diameters larger than 0.56 mm (Jarvis and Larsbo 2023). Additionally, water content at field capacity (θ_{FC}, at 100 hPa suction) was measured on 922 soil cores (111 plots, 2 to 3 depths, 1 to 4 soil cores per plot) using HYPROP2 (Meter Group GmbH, Germany) for 250 cm^3 soil cores ($n=251$) and suction plates (e.g., ecoTech Umwelt-Messsysteme GmbH, Germany) for 100 cm^3 soil cores ($n=671$), and bulk density (BD) was determined by oven drying at 105°C for 48 h. 316 composite soil samples (111 plots, 2 to 3 depths) were analysed for texture (pipette method) and SOC content (dry combustion, or wet oxidation with dichromate for Swiss LTEs). Water stable aggregates index (WSA) was determined on 300 of these soil samples with triplicates (technical replicates) per sample (Nimmo and Perkins 2002). Particle density (PD) was measured with the pycnometer method on 249 soil samples from all plots and depths, except for BOPA (Belgium), where PD was estimated with the pedotransfer function from Schjønning et al. (2017), assuming soil organic matter content to be double the measured SOC (Pribyl 2010):

$$\mathrm{PD}\ \left[\mathrm{Mg\ m^{-3}}\right] = \left(\frac{2*\mathrm{SOC}\ \left[\mathrm{kg\ kg^{-1}}\right]}{1.127+0.746*\mathrm{SOC}\ \left[\mathrm{kg\ kg^{-1}}\right]} + \frac{1-2*\mathrm{SOC}\ \left[\mathrm{kg\ kg^{-1}}\right]}{2.648+0.209*\mathrm{clay}\ \left[\mathrm{kg\ kg^{-1}}\right]} \right)^{-1} \quad (1)$$

All data obtained from all plots of the ten LTEs were collected with spreadsheet templates, compiled into a single dataset that is available on Zenodo (Heller, ten Damme, et al. 2024), and prepared for statistical analyses as described below.

2.3 | Data Analyses

All data processing and statistical analysis were performed using the free and open source statistical software R (version 4.5.2; R Core Team 2024), with several extension packages including glmm.hp (Lai et al. 2023), lme4 (Bates et al. 2015), lmerTest (Kuznetsova et al. 2017), MuMIn (Bartoń 2024), piecewiseSEM (Lefcheck 2016), relaimpo (Groemping 2007), SoilHyP (Dettmann 2023), SoilManageR (Heller et al. 2025) and soiltexture (Moeys 2024).

2.3.1 | Data Harmonisation and Transformation

For the analyses, we included the 92 plots for which all soil properties were available for the topsoil (10 cm depth, 5 cm depth for BOPA) and the subsoil (30 cm depth, 45 cm depth for BOPA) (see Table 1 for excluded treatments). To account for methodological differences between wet oxidation (SOC_{wo}) and dry combustion (SOC_{dc}), we applied a correction factor of $SOC_{dc} = 1.18 \times SOC_{wo}$ for the Swiss SOC data, based on findings from 105 Swiss soils (Gubler et al. 2018). Soil texture data from Austria, Denmark and Sweden were converted to USDA soil textural classes (clay $< 2\,\mu m \leq$ silt $< 50\,\mu m \leq$ sand < 2 mm $<$ gravel; Soil Science Division Staff 2017) using a log-linear transformation (Nemes et al. 1999).

Gravimetric soil water content at the permanent wilting point (15,000 hPa suction, w_{PWP}) was calculated using the pedotransfer function from Seybold and Harms (2012), given in Equation (2).

$$w_{PWP}\,[\%] = 0.406 * \text{clay}\,[\%] + 0.752 * \text{SOC}\,[\%] \tag{2}$$

Multiplying w_{PWP} by the gravel-corrected BD and dividing by the density of water ($\rho_{H_2O} = 1\,\text{Mg}\,\text{m}^{-3}$) gave the volumetric water content at the permanent wilting point (θ_{PWP}). Plant-available water (PAW) per unit mass was calculated as:

$$\text{PAW} = \frac{(\theta_{FC} - \theta_{PWP}) * \rho_{H_2O}}{\text{BD}} \tag{3}$$

Porosity was derived from BD and PD, and air capacity (AC) at 100 hPa suction was determined as the difference between porosity and θ_{FC}. For analyses, K_{sat} and K_{5hPa} were $\log_{10}$-transformed and earthworm abundance was square root transformed. One representative value per plot and depth was obtained by calculating the arithmetic mean (after transformation) of all soil core derived measures, FPR, WSA, VESS and earthworm.

Since there were differences across laboratories for some methods, we tested for methodological effects, also considering possible laboratory effects (Table S1). In brief, we found significantly lower values for K_{sat}, K_{5hPa} and PAW as well as higher BD values measured on the 100 cm^3 soil cores compared to values from the 250 cm^3 soil cores. In the subsequent analysis we accounted for these methodological sources of variation explicitly by a fixed effect for the method in the linear models, or implicitly by including a random effect structure that accounts for methodological effects in the mixed-effect models.

2.3.2 | Correlation Analysis for Soil Physical Properties

A correlation analysis for all measured soil physical properties was performed (Figure S1) to identify general patterns in the dataset. Based on the identified correlations and existing knowledge (Pachepsky and Rawls 2004; Zhang and Schaap 2017; Szabó et al. 2021; Weber et al. 2024), we selected BD, SOC, clay and sand as potential predictors to explain differences in soil physical properties (PAW, AC, K_{sat}, K_{5hPa}, FPR, WSA, BD and VESS) in linear regression models (Table 2, Figures 4 and 5). We performed stepwise backward model selection and retained only predictors with p-values below 0.1 in the models and calculated the relative importance of the predictors by averaging over orderings (Groemping 2007). For the linear models, we assumed all our observations to be independent (i.e., $N = 184$; 92 per depth). The observations were weighted to avoid LTEs with more blocks or treatments unduly influencing the model estimates. A weighting factor inversely proportional to the number of plots in each LTE was assigned to each observation, such that all LTEs received the same total weight of one. We checked for correlation between predictor variables (Fox and Monette 1992) and found no relevant correlation (all variance inflation factors were below 2.3).

2.3.3 | Variability of Soil Properties Between LTEs and Treatments

First, a series of sequential ANOVAs for each explanatory and dependent variable was conducted to assess the variability that occurred at the LTE-level, at the treatment-level and at the plot level (Table S2). Second, we calculated treatment means and standard deviations for each of the soil properties (VESS, earthworm, BD, SOC, PAW, AC, K_{sat}, K_{5hPa}, FPR, WSA) for each LTE and depth separately. Treatment effects on soil properties were statistically analysed with 180 factorial ANOVAs (10 LTEs, 18 soil properties) that accounted for possible block effects (Table S3). While these two approaches allowed to reveal the relative contribution of the site (i.e., the LTEs) versus the management (i.e., the treatments) and answer the question how much soil properties differ at a specific site due to management, they do not allow to quantify the effect of management intensities and pedo-climatic context.

2.3.4 | Direct and Indirect Effects of Management and Pedo-Climatic Conditions on Soil Properties

The direct effects of soil management intensity (C input, STIR and N_{min} input) and the pedo-climatic context (clay, sand, MAT and MAP) on each measured soil property were investigated with linear mixed-effect models. The measured soil properties shown in Figure 1 were grouped into moderators (earthworms, SOC, BD) and physical properties (K_{sat}, K_{5hPa}, PAW, AC, WSA, FPR and VESS). For each soil property at each depth, separate models were run that included the three

TABLE 2 | Estimated coefficients of the final linear models (after stepwise backward variable selection) that determine soil physical properties from bulk density (BD), soil organic carbon (SOC), soil texture and soil core size (CS).

Soil physical property	Model estimates (and relative importance)						Adjusted R^2
Plant available water (PAW)	0.454***	−0.168***· BD	+0.003***· SOC	−0.004***· clay	−0.001***· sand	−0.011**· CS	0.79
$N=184$		(44%)	(34%)	(14%)	(4%)	(3%)	
Air capacity (AC)	0.656***	−0.352***· BD	−0.006***· SOC		+0.001***· sand		0.56
$N=184$		(70%)	(20%)		(9%)		
$\log_{10}(K_{5hPa})$	3.448***	−2.137***· BD	−0.06***· SOC	+0.024**· clay	+0.011***· sand	−0.255**· CS	0.29
$N=184$		(23%)	(31%)	(10%)	(15%)	(21%)	
$\log_{10}(K_{sat})$	4.582***	−1.858***· BD			−0.004· sand	−0.182*· CS	0.25
$N=184$		(68%)			(15%)	(17%)	
Field penetration resistance (FPR)	−4.533***	+3.827***· BD		+0.068***· clay			0.22
$N=179$		(66%)		(34%)			
Water stable aggregate index (WSA)	0.200**		+0.018***· SOC	−0.005**· clay	+0.004***· sand		0.44
$N=184$			(50%)	(18%)	(32%)		
Bulk density (BD)	1.612***		−0.018***· SOC		+0.001*· sand	+0.044**· CS	0.54
$N=184$			(81%)		(9%)	(9%)	
Visual soil evaluation score (VESS)	2.174***		+0.043***· SOC	−0.023*· clay			0.14
$N=92$			(70%)	(30%)			

Note: CS was excluded from the initial models for FPR, WSA and VESS, and BD was excluded for the initial BD model. For the analysis, VESS scores were inverted (higher values are a better score). Values in brackets indicate the relative importance of the variable within the respective linear model. The relative importance for each model sums up to 100%. Units: PAW (kg kg^{-1}), AC (m^3 m^{-3}), K (cm day^{-1}), WSA (–), FPR (MPa), BD (Mg m^{-3}), clay (%), sand (%), SOC (gC kg^{-1}), VESS (–). CS = 1 if small soil cores (100 cm^3) and suction tables were used ($n=112$), 0 if large soil cores (250 cm^3) and HYPROP2 were used ($n=88$). Significance codes: p-value = 0.1 ≥ · > 0.05 ≥ * > 0.01 ≥ ** > 0.001 ≥ ***.

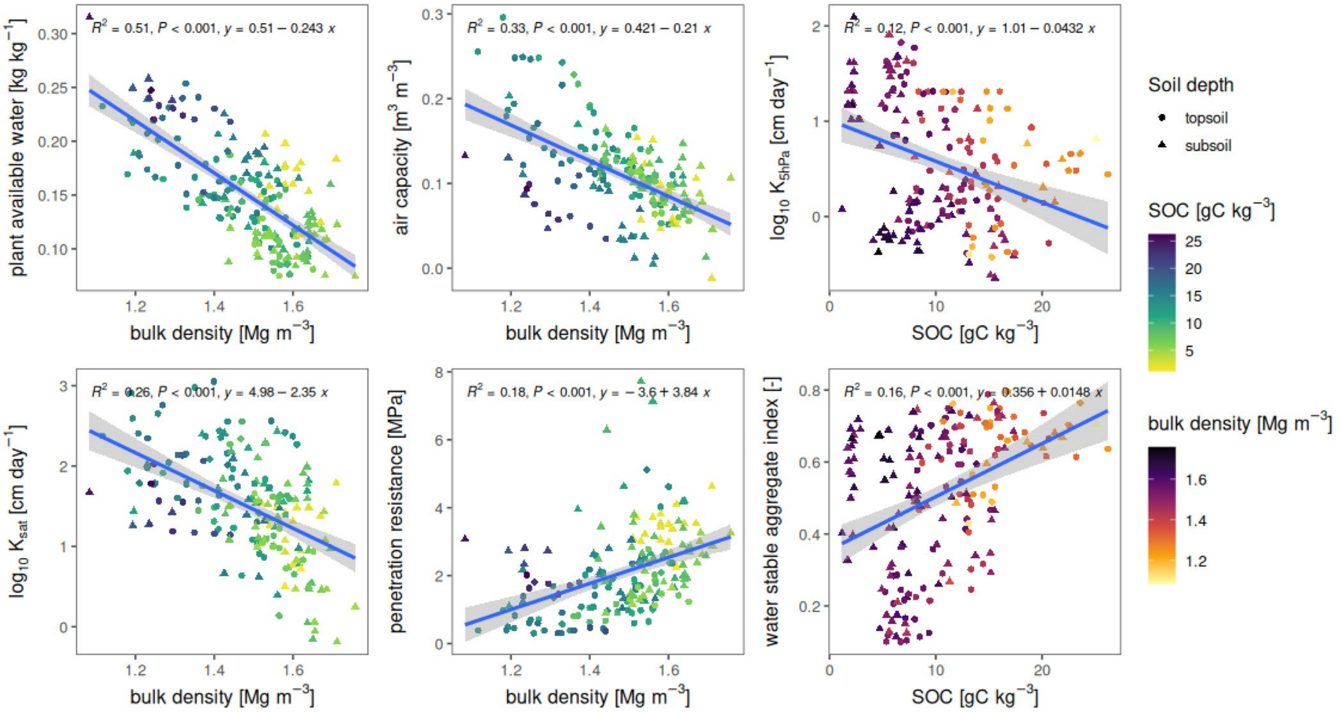

FIGURE 4 | Scatterplots of the soil physical properties—gravimetric plant available water (PAW), air capacity (AC), hydraulic conductivity of the soil matrix (K_{5hPa}) and the macropores (K_{sat}), field penetration resistance (FPR) and water stable aggregate index (WSA)—as a function of soil organic carbon content (SOC) if SOC was the most important predictor and as a function of bulk density (BD) if BD was the most important predictor (see Table 2). Each data point represents the average of one to three measurements per plot and depth. Colours highlight levels of SOC or BD. Regression lines and statistics in the plots only refer to the soil property on the *x*-axis and differ from the linear models in Table 2.

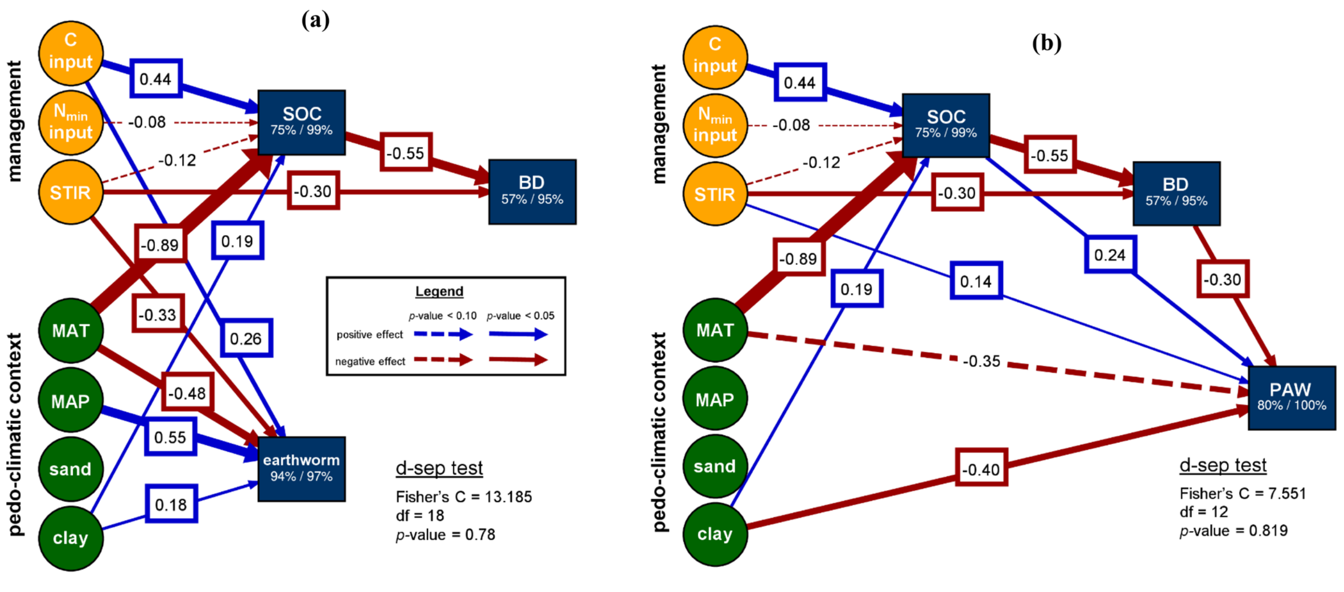

FIGURE 5 | Piecewise structural equation model diagrams show the direct and indirect effects of soil management (yellow circles) and pedo-climatic context (green circles) on soil properties (blue boxes) in the topsoil. (a) The effects of management and pedo-climatic context on the mediating soil properties SOC, BD and earthworm. (b) The direct and indirect effects of management and pedo-climatic context on plant available water (PAW). Arrow thickness and number associated with it represent standardised effect sizes. The %-values in the blue boxes refer to the marginal and the conditional pseudo R^2 of the final mixed-effect model for the respective soil property (see Table 3). Path analysis diagrams for all other variables can be found in Figures S2–S14. BD, bulk density; C, carbon; df, degrees of freedom; MAP, mean annual precipitation sum; MAT, mean annual temperature; N, nitrogen; PAW, gravimetric plant available water; SOC, soil organic carbon; STIR, soil tillage intensity rating.

soil management indicators and the four pedo-climatic indicators as potential predictor variables. We further included SOC and earthworm as potential moderators for the model for BD, and in the models for the physical properties we included all three moderators as potential predictors. Each model included a random effect for the LTE to represent the structured nature

TABLE 3 | Estimated coefficients of the final mixed-effect linear models (after backward variable selection) that estimate the dependence of soil physical, chemical and biological properties from management intensities, pedo-climatic context and mediating soil properties (SOC, BD and earthworm).

	Model estimates										Pseudo R^2	
Soil property	**Intercept**	**C input**	**STIR**	**N_{min} input**	**MAP**	**MAT**	**Clay**	**Sand**	**SOC**	**BD**	**Marg.**	**Cond.**
$\sqrt{(\text{earthworm})}$	11.2809*	0.8801**	−0.0338***		0.0144**	−1.4095**	0.1900*			—	0.94	0.97
		(9%)	(9%)		(43%)	(30%)	(3%)					
VESS score	4.3372***		−0.0027*							−1.1978*	0.21	0.89
			(12%)							(9%)		
Topsoil												
SOC	27.8695***	1.0548***	−0.0082·	−0.0102·		−1.8139**	0.1398*		—	—	0.75	0.99
		(7%)	(1%)	(0%)		(64%)	(3%)					
BD	1.6879***		−0.0006**						−0.0156***	—	0.57	0.95
			(14%)						(43%)			
PAW	0.399***		0.0001**			−0.0073·	−0.0031***		0.0024***	−0.1097***	0.8	1.00
			(3%)			(39%)	(12%)		(10%)	(16%)		
AC	0.8452***		−0.0002***					0.001**	−0.0062***	−0.4706***	0.69	0.99
			(1%)					(12%)	(7%)	(49%)		
$\log_{10}(K_{sat})$	6.5243***		−0.0036**				0.029·		−0.0471*	−2.975***	0.44	0.93
			(10%)				(6%)		(0%)	(28%)		
$\log_{10}(K_{5hPa})$	−0.7944					0.1657*	0.0223·	0.0106·		−0.895*	0.52	0.97
						(41%)	(4%)	(4%)		(3%)		
FPR	−0.0394		−0.0096***							1.7006**	0.51	0.99
			(38%)							(13%)		
WSA	0.9153***	0.0427***	−0.0004*			−0.0593**		0.0029*			0.76	0.99
		(18%)	(−1%)			(50%)		(8%)				
Subsoil												
SOC	34.9885***				−0.0086·	−1.9243**			—	—	0.63	0.98
					(11%)	(52%)						

(Continues)

TABLE 3 | (Continued)

	Model estimates										Pseudo R^2	
Soil property	**Intercept**	**C input**	**STIR**	**N_{min} input**	**MAP**	**MAT**	**Clay**	**Sand**	**SOC**	**BD**	**Marg.**	**Cond.**
BD	1.5369***							0.0022·	−0.0116***	—	0.49	0.96
								(12%)	(37%)			
PAW	0.4185***						−0.0025***		0.0023***	−0.1665***	0.58	0.99
							(7%)		(22%)	(29%)		
AC	0.7472***						−0.0025**		−0.0044***	−0.3764***	0.45	0.99
							(0%)		(3%)	(42%)		
$\log_{10}(K_{sat})$	3.0101***			0.0043**	−0.0011·					−0.8577·	0.4	0.96
				(8%)	(27%)					(5%)		
$\log_{10}(K_{5hPa})$	0.7572					0.2267**		0.0113*		−2.1283***	0.66	0.98
						(42%)		(4%)		(20%)		
FPR	3.0161***	0.1919*	−0.0093***								0.23	0.97
		(11%)	(11%)									
WSA	0.9426***					−0.0609***		0.0041**			0.86	0.96
						(70%)		(16%)				

Note: Values in parentheses represent the relative importance of the variable to explain the total variability, that is, they sum up to the marginal pseudo R^2. For the analysis, VESS scores were inverted (higher values are a better score). The number of observations was the same for all models (N = 92). Earthworm was not selected as a relevant predictor variable in any final model and was omitted from the table head. Units: Plant available water (PAW) ($kg\,kg^{-1}$), Air capacity (AC) ($m^3\,m^{-3}$), hydraulic conductivities (K) ($cm\,day^{-1}$), Water stable aggregate index (WSA) (–), Field penetration resistance (FPR) (MPa), Bulk density (BD) ($Mg\,m^{-3}$), clay (%), sand (%), soil organic carbon (SOC) ($gC\,kg^{-1}$), VESS score (–), earthworms ($\#\,m^{-2}$), C input ($Mg\,C\,ha^{-1}\,year^{-1}$), STIR ($year^{-1}$), N_{min} input ($kg\,N\,ha^{-1}\,year^{-1}$), mean annual precipitation sum (MAP) (mm), mean annual temperature (MAT) (°C). Significance codes: p-value = 0.1 ≥ · > 0.05 ≥ * > 0.01 ≥ ** > 0.001 ≥ ***. —: This variable was not included in the full model.

of our dataset and to account for methodological effects. As for the linear models (see Section 2.3.2), we weighted the observations, performed stepwise backward model selection, and checked for correlation between predictor variables. Again, no relevant correlation was found as all variance inflation factors were below 1.6. To rank the relative importance of each predictor variable, we used hierarchical variance partitioning (Lai et al. 2023). The relative importance of each predictor variable for eight response variables (SOC, BD, PAW, AC, K_{5hPa}, K_{sat}, FPR and WSA) was averaged to quantitatively summarise the relative importance of each predictor variable in the topsoil and the subsoil separately. We assessed the robustness of the statistical analyses by performing an iterative leave-one-group-out (LOGO) analysis (Tables S4 and S5). In each iteration of the LOGO analysis, data from one LTE was left out from the dataset and the refitted model parameters were compared to the parameters from the full models. To explore potential nonlinear relationships between explanatory variables and soil properties, we conducted exploratory analyses (section 10 in Appendix S1, Figure S21). These nonlinear analyses were not part of the original study design and are therefore interpreted cautiously.

We applied path analysis to capture indirect effects of management and pedo-climatic context (Grace 2006; Eisenhauer et al. 2015). For this path analysis, the final models were combined into a set of unidirectional piecewise structural equation models (pSEM; Lefcheck 2016) to assess and visualise the indirect effects of soil management and pedo-climatic context through mediating soil properties (Figures 5; and Figures S2–S14). pSEM were chosen over traditional SEMs because they allow us to represent hierarchical data structures (i.e., plots nested in LTEs). The pSEM model fits were assessed by Shipley's *d*-sep tests (Shipley 2009).

3 | Results

3.1 | Soil Physical Properties Depend on Soil Texture, SOC and Bulk Density

The present study confirmed robust negative correlations ($r < -0.5$) between BD and several other soil physical properties including PAW ($r = -0.71$), SOC ($r = -0.69$), AC ($r = -0.57$) and K_{sat} ($r = -0.51$). A strong positive correlation was found between PAW and SOC ($r = 0.63$), as shown in Figure S1. The strong correlations between SOC, BD and soil physical properties across topsoil and subsoil were also reflected in the relative importance of the predictors in the linear regression models (Table 2, Figure S15). BD alone accounted for more than 65% of the explained variation in AC, K_{sat} and FPR. It has been established that soils with higher BD exhibit lower AC, lower K_{sat} and higher FPR. The combination of SOC and BD explained 78% and 54% of the variation in PAW and K_{5hPa}, respectively. PAW was enhanced in soils with reduced BD and increased SOC, whereas the matrix hydraulic conductivity (K_{5hPa}) was higher in soils with lower BD and reduced SOC. The variability in WSA and VESS was attributed solely to the combination of SOC and soil texture. WSA was higher and VESS score was better in soils with more SOC and less clay. Furthermore, WSA was found to be higher in soils with a greater proportion of sand. Figure 4 shows the soil physical properties in relation to the most relevant explanatory variables of the linear models in Table 2 (BD or SOC).

3.2 | Stronger Site Effects in the Subsoil Than the Topsoil

Attributing variability to the different levels of our dataset (Table S2) revealed that for all but three variables (N_{min} input, K_{sat} in the topsoil and AC in the subsoil), differences between sites (i.e., the LTEs) were larger than within sites. Management indicators for C input and STIR showed between-site variability of 81% and 61%, respectively. As a result, topsoil properties mostly depended on the site (more than 75% of the variability in PAW, WSA, SOC, earthworm and K_{5hPa}). The relative variability explained by site was slightly lower for FPR and BD (73% and 67%, respectively) while for the VESS score it was 52% and for K_{sat} it was 46%. The variabilities in topsoil properties explained by the treatments were comparably low (3%–20%). In the subsoil, the proportion of the variability explained by the site was higher than in the topsoil. For all subsoil properties, the variabilities explained by the site were > 75%, except for BD (73%), K_{sat} (64%) and AC (32%). Consequently, variabilities attributed to the treatments (2%–13%) were lower in the subsoil than in the topsoil.

In line with these findings, the series of 180 LTE-specific ANOVAs (Table S3) revealed only 40 significant treatment differences, of which 23 were strongly significant (p-value < 0.05) and 17 were weakly significant (p-value < 0.1). Thirty significant differences occurred in the topsoil and ten in the subsoil. Most differences were found for FPR ($n = 10$), followed by SOC ($n = 8$), BD ($n = 5$), earthworm abundance ($n = 4$) and WSA ($n = 4$). More trends could be observed when treatment means are compared, but due to high variability between plots, most differences were not statistically significant.

3.3 | Mixed-Effect Models Linked Drivers, Moderators and Soil Physical Properties

As expected, the mixed-effect models (Table 3) that accounted for soil management and pedo-climatic context explained differences in soil physical properties better than the linear models that only considered soil properties. The linear models had an average adjusted R^2 of 43% (Table 2), whereas the mixed models (Table 3) for the topsoil had an average marginal R^2 of 62% and those for the subsoil had an average marginal R^2 of 53%. The marginal R^2 of the mixed models refers to the proportion of the total variability explained by the fixed effects alone, whereas the conditional R^2 also includes the proportion of the variability explained by the random effect (i.e., the site). The models for explaining earthworm, topsoil SOC, topsoil PAW as well as topsoil and subsoil WSA showed the best fits (marginal $R^2 \geq 0.75$). The models for VESS score and subsoil FPR fitted the data poorly (marginal $R^2 < 0.25$). However, when unknown site effects such as observer effects for VESS scores, soil moisture content for FPR, and differences in equipment and methods were accounted for, the R^2 of all models increased to above 0.89 (see conditional R^2 in Table 3). The refitting of the models with iteratively omitting the data from one site in the LOGO analysis (Tables S5 and S6) showed that our mixed-effect model estimates were robust.

The mediating soil properties were well explained by the models (Figure 5a, Table 3 and Figures S16 and S17): earthworms were more abundant in plots with high MAP, low MAT, high C input, low STIR and high clay content. Topsoil SOC was higher for plots with low MAT, high C inputs, high clay contents and low STIR and N_{min} input values. Topsoil BD, in turn, was highest in plots with low SOC and low STIR. The soil physical properties were dependent on combinations of pedo-climatic context, management intensities and mediating soil properties (Table 3, Figure S17). It is noteworthy that while topsoil SOC and BD were significant moderators mediating the physical properties, earthworm abundance did not appear to mediate any of the physical properties.

3.4 | Path Analysis Revealed Direct and Indirect Effects

The pSEMs visualise the direct and indirect effects of the pedo-climatic and management indicators on the soil physical properties (Figure 5 and Figures S2–S14). Overall, the pSEM models showed good fits (d-sep test $p > 0.1$) for all variables, except for FPR. The FPR models for the topsoil and the subsoil fitted the data poorly (d-sep test $p < 0.1$, Figures S10 and S11), suggesting missing pathways or variables. Further investigation with a reduced dataset that included the degree of the soils water saturation at the time of sampling showed much better model fit (Figures S18 and S19). Related to this, the topsoil FPR pSEM of the reduced dataset had a d-sep test result of $p = 0.14$ (pSEM not shown). However, the water content at sampling was not available for all sites and could therefore not be included in the full model.

Figure 5b illustrates that PAW was directly affected by the pedo-climatic context (lowered by high MAT and high clay contents) and soil management (increased by higher STIR). Additionally, PAW was also indirectly affected by the impacts of MAT and C input on SOC contents and BD. Across all 14 pSEMs (Figure 5; and Figure S2–S14), several consistent patterns emerged. In many cases, MAT and C input influenced soil physical properties mainly indirectly through their effects on SOC rather than through direct pathways. In contrast, tillage intensity affected topsoil physical properties both directly and indirectly through BD. Overall, management effects—whether direct or indirect—were generally weaker in the subsoil compared to the topsoil.

3.5 | Pedo-Climatic Context Was More Important Than Management

The effect of the pedo-climatic context dominated over the impacts of management practices, as shown by averaging the relative importances of the explanatory variables in Table 3. In the topsoil, the average relative importance of the pedo-climatic context (MAP, MAT, clay, sand) on eight response variables (SOC, BD, PAW, AC, K_{5hPa}, K_{sat}, FPR and WSA) was 30.4%, compared to 11.4% for the management drivers (C input, STIR and N_{min} input). This is roughly a ratio of 3:1 for the variability in soil properties explained by pedo-climatic context relative to the variability explained by management. In the subsoil, the predominance of the pedo-climatic context was more pronounced: 30.1% for pedo-climate versus 3.8% for management (i.e., a ratio of 8:1). Discrimination between climatic context (MAP, MAT), pedological context (clay, sand) and management drivers (C input, STIR, N_{min} input) resulted in ratios of 2:1:1 (climate: texture: management) for the topsoil and 7:1:1 for the subsoil.

4 | Discussion

4.1 | Topsoil SOC, BD and Earthworm Abundance Respond to C Inputs and Tillage Intensity

Our piecewise SEMs suggest that the effect of C input and tillage intensity on topsoil properties was often mediated through SOC and BD. SOC increased with higher C inputs but declined slightly with increasing STIR and N_{min} inputs. MAT was the most important pedo-climatic predictor for SOC (Figure 5b), consistent with faster organic matter decomposition under warmer climates (Cotrufo and Lavallee 2022; Wiesmeier et al. 2019; Hartley et al. 2021). Exploratory nonlinear analyses (Figure S21) further indicated that SOC declines were mainly associated with very high tillage intensity and N_{min} inputs, whereas temperature effects were strongest under colder conditions. These exploratory findings should be interpreted cautiously but may help reconcile contrasting observations regarding SOC response to mineral fertilisation (Poffenbarger et al. 2017; Tang et al. 2025). The nonlinear temperature response is also consistent with declining decomposition sensitivity at higher temperatures (Kirschbaum 1995).

As commonly observed (Strudley et al. 2008; Lal 2020), BD was lower in soils with higher SOC content and decreased with higher tillage intensity. These management-induced changes in SOC and BD propagated into most other soil physical properties, suggesting that SOC and BD may serve as practical proxy indicators in broad-scale assessments or monitoring contexts where more comprehensive soil physical measurements are not feasible.

The findings that higher C inputs and lower STIR increased earthworm abundance, and that higher MAP, lower MAT and greater clay contents were associated with more earthworms are consistent with knowledge about earthworm habitat preferences and management impacts (e.g., Briones and Schmidt 2017; Phillips et al. 2019; Simon et al. 2025; Sturm et al. 2026). However, contrary to our initial assumption and previous literature linking earthworms to soil structure formation (e.g., Capowiez et al. 2009; Blouin et al. 2013), earthworm abundance was not identified as a significant mediator of soil physical properties. This may reflect shared responses of earthworm abundance and soil properties to the same pedo-climatic and management drivers. In addition, our statistical analysis did not explicitly consider functional differences among earthworm communities, which are known to differ in their effects on soil structure (Andriuzzi et al. 2015; Capowiez et al. 2024).

4.1.1 | Water Storage Is Enhanced by SOC and Low BD, but Higher Tillage Intensity Reduces Infiltration

Management influenced soil water storage mostly indirectly through effects on SOC and BD. Higher C inputs enhanced SOC, which increased PAW, while reduced tillage intensity increased BD and thereby lowered PAW. The linear models estimated a 1.7$\%_{mass}$ increase in gravimetric PAW per 0.1 Mg m^{-3} decrease in BD, and a 3$\%_{mass}$ increase per 10 g kg^{-1} increase in SOC. Accounting for the positive SOC–BD relationship approximately doubled the estimated SOC effect on PAW to ~6$\%_{mass}$ per 10 g C kg^{-1} SOC (Table 2). For a typical arable topsoil, such an increase may correspond to roughly 4–5 additional days of crop water supply during summer conditions in temperate climates (Liu et al. 2002). Previous studies that did not account for this SOC-BD coupling generally reported smaller effects of SOC on PAW (e.g., Libohova et al. 2018; Minasny and McBratney 2018).

Infiltration characteristics were also affected by soil management. K_{sat} decreased strongly with increasing BD, reflecting a loss of macropores (Archer and Smith 1972). K_{sat} was also reduced directly under high tillage intensity (Figure S8), likely due to the destruction of continuous biopores (Jarvis 2007; Schlüter et al. 2020). The contrasting effects of tillage on K_{sat} likely reflect a trade-off between transient tillage-induced macropores and the preservation of stable biopores under reduced tillage. As expected, K_{5hPa} was less dependent on BD but more dependent on soil texture and SOC than K_{sat}. Both K_{sat} and K_{5hPa} were unexpectedly reduced at higher SOC contents, which may reflect water repellency and water retention of soil organic matter or pore clogging (Nemes et al. 2005; Jarvis et al. 2013).

4.1.2 | Erosion Resistance Is Enhanced by Higher C Input and by Reduced Tillage

Aggregate stability in the topsoil, a key indicator for soil resistance to erosion (Barthès and Roose 2002; Holz et al. 2015), was enhanced by higher C inputs and by reduced tillage intensity, which is in agreement with Amézketa (1999), Six et al. (2004), Abiven et al. (2009) and Seitz et al. (2019). However, MAT emerged as the most important predictor for aggregate stability, possibly due to its strong effect on organic matter turnover. In our data, topsoil WSA increased with SOC up to a SOC level of approximately 16.5 g kg^{-1} (Figure S20), a value slightly below the threshold for aggregate stability of 20 g kg^{-1} SOC reported by Kay and Angers (2001). According to our SOC model (Table 3), an average annual C input of about 7.1 Mg per hectare is needed to reach 16.5 g kg^{-1} SOC for the hypothetical average site in our dataset (Table S2), while higher C inputs would be needed at sites with warmer climate and lower clay content.

Low infiltration capacity can further increase erosion risk through surface runoff (Holz et al. 2015). As discussed above for K_{sat}, management influenced infiltration characteristics through interacting effects on BD and biopore continuity. Together with the observed effects on aggregate stability, this indicates that management influences erosion resistance, although these effects vary with the time since last tillage operations (Blanchy, Albrecht, et al. 2023).

4.1.3 | Soil Aeration and Penetration Resistance Are Driven by Bulk Density

Soil aeration was strongly controlled by BD, confirming the well-known inverse relationship between soil compactness and aeration (Archer and Smith 1972; Stepniewski et al. 1994). Nevertheless, an unexpected pattern emerged: similar to the trend observed for K_{sat} but opposite to BD, AC tended to be lower under higher tillage intensity. This pattern may be the result of sampling consolidated soil in which tillage-induced macropores that enhanced soil aeration had already collapsed.

Soil penetrability by roots, as approximated by FPR, was generally higher with increased tillage intensity (Figure 3) as soil loosening decreases soil strength and BD. In the plots with higher C inputs, subsoil FPR was increased in some LTEs, which may be a result of soil compaction caused by additional machinery passes needed to apply organic amendments (ten Damme et al. 2021). The strong site effect for FPR likely reflects the differences in soil moisture conditions at sampling (Figure S18), as FPR generally increases under drier conditions (Hernanz et al. 2000; Dexter et al. 2007). Including soil moisture improved the performance of our model, confirming its relevance as a driver of FPR (see Section 3.4 and Figure S19), but it was not available for all sites and therefore not included in the main analysis.

4.2 | Stronger Impact of Pedo-Climate Than Management

The overshadowing role of pedo-climatic conditions compared to management effects in our dataset is consistent with findings of other continental-scale studies in Europe (e.g., Garland et al. 2021; Smith et al. 2021; Edlinger et al. 2023; ten Damme et al. 2025), emphasising that site-dependent conditions largely determine soil (physical) properties. The climate-induced differences in topsoil SOC propagated into nearly all soil physical properties that were measured, reflecting the central role of SOC (Blanco-Canqui et al. 2013). Climatic conditions regulate both the accumulation and decomposition of organic matter, while soil texture determines the capacity of soils to form SOC protecting structure (Cotrufo and Lavallee 2022; Wiesmeier et al. 2019). As a consequence, sites with low clay content or warm climates have limited capacity to build up SOC (Davidson and Janssens 2006) and improve soil structure, even under improved management practices. From a climate change adaptation perspective, these findings imply that adapted soil management strategies may not be able to fully compensate the effect of increasing temperatures on soil physical properties, especially in fast warming regions and coarse-textured soils. On such sites, soil management should focus to buffer crop production declines under drought periods by changing water fluxes (Heitman et al. 2023) in addition to improving relevant soil physical properties. For example, by leaving crop residues on the soil surface to reduce bare soil evaporation (Ramos et al. 2024).

4.3 | Limited Impact of Management on Subsoil Properties

In the topsoil, pedo-climatic conditions dominated over management influences by a ratio of 3:1, indicating that agricultural management provides some scope to modify topsoil physical properties. In the subsoil, the dominance of pedo-climatic conditions increased to a ratio of 8:1, suggesting that the management practices investigated in this study had limited influence on subsoil physical properties.

A key reason for this limited influence is that most management interventions, particularly tillage, primarily affect the soil within the plough layer and therefore have little direct influence on deeper soil layers. If anything, direct subsoil effects may be negative, for example through subsoil compaction caused by machinery traffic or in-furrow ploughing (Alakukku et al. 2003; Chamen et al. 2003). Consequently, management effects on subsoils are predominantly indirect and mediated through processes such as the vertical distribution of root biomass, soil faunal activity and the transfer of organic matter to the subsoil. However, the inputs of organic matter to deeper soil layers are generally limited and turnover rates are slower compared to the topsoil (Dungait et al. 2012; Balesdent et al. 2017).

As a consequence, subsoil physical properties are largely governed by persistent site-specific features such as clay mineralogy and local hydrology, along with only partially manageable structures like biopore networks formed by roots and soil fauna (Lucas et al. 2019). Addressing these constraints, which limit the responsiveness of subsoil properties to management, may require more targeted and intensive management interventions than the ones that were applied in the 10 LTEs of our study. Such interventions should aim to increase the transfer of organic carbon and biological activity to deeper soil layers (Lorenz and Lal 2005). Practices that promote deeper rooting systems, such as deep-rooting cover crops and cultivars (Heinemann et al. 2023), perennial crops and pastures (McCallum et al. 2004) or agroforestry systems (Cardinael et al. 2018), may help deliver more root biomass and exudates to deeper soil layers and thereby improve their physical properties. Management practices that promote soil fauna, particularly anecic earthworms, may enhance subsoil structure by creating continuous macropores (Francis and Fraser 1998; Capowiez et al. 2009) and transporting organic residues to deeper soil layers (Kuzyakov and Kooch 2024; Kautz 2015). Targeted deep tillage operations may provide a means to directly modify subsoil structure (McBeath et al. 2026; Geers-Lucas et al. 2025), although such operations should be promoted and applied with caution to avoid unintended side-effects, such as subsequent compaction (Schneider et al. 2017). In addition, avoiding subsoil compaction is critical, as it is often an unintended consequence of management and can strongly impair soil functioning while being difficult to reverse (Chamen et al. 2003; Keller et al. 2019).

4.4 | From Continental-Scale Studies to Context-Specific Recommendations

While continental-scale studies like ours primarily identify general patterns, they also provide a basis for developing more context-specific recommendations for farmers, advisers and policymakers. For example, our results suggest that increasing C inputs may be particularly effective in cooler regions and clay-rich soils, where higher SOC stabilisation potential can lead to more pronounced improvements in soil physical properties. The considerable heterogeneity in climates, soils and sampling conditions across Europe naturally introduced variation into our dataset. However, the heterogeneity can also be viewed as a resource for cross-regional learning. As climate change modifies temperature and precipitation regimes, management strategies established in warmer and drier regions of Europe may inform adaptation in regions experiencing comparable conditions in the future.

Applicable recommendations require studies that focus on local pedo-climatic conditions where management has a stronger influence on soil properties relative to environmental constraints (e.g., Garland et al. 2021; Heller et al. 2025) and where findings are more easily transferable to practice (Thorsøe et al. 2023). By combining soil management indicators with mixed models and path analysis, our study provides a framework for such future studies with regional scope within comparable climatic conditions. In addition, our exploratory analyses (Figure S21) suggest that the response of soil properties to explanatory variables may be nonlinear, highlighting the need for more flexible modelling approaches. Statistical advances such as generalised additive models or machine learning can help capture those nonlinear responses and account for interactions among drivers (e.g., Nyaupane et al. 2024; Klöffel et al. 2024). Future analyses should also consider trade-offs with agronomic outcomes, such as crop productivity (Roel-Rezk et al. 2025), since improvements in soil properties do not automatically lead to improved crop productivity or farm profitability (Miner et al. 2020; Wittwer et al. 2021).

5 | Conclusions

Our analysis of 10 long-term field experiments across Europe shows that although pedo-climatic context dominates, soil management influences the soil hydraulic and mechanical properties of arable soils. In particular, C inputs and tillage intensity (STIR) influence SOC, BD, earthworm abundance and soil structure, thereby affecting water regulation, erosion resistance, soil aeration and penetrability. Our results also indicate that the effects of the investigated management interventions below the topsoil were limited.

These findings provide a framework for context-specific soil management advice. While increased C input and reduced tillage intensity can improve soil physical properties, their effectiveness depends strongly on pedo-climatic context. In dry and warm environments, management alone may not be sufficient to improve soil physical properties, indicating that broader adjustments in soil and land use may be required. By quantifying the relative importance of management and pedo-climatic controls, our study helps to identify where management interventions are most effective and where inherent pedo-climatic constraints dominate. This highlights the need to tailor soil management strategies to local conditions rather than relying on generalised recommendations. Embedding these context-specific insights in regional analyses and linking them to yield responses can further support the optimisation of soil functions for climate-resilient cropping systems.

Acknowledgements

We gratefully acknowledge the contributions of all partners and collaborators who supported the development of the presented dataset and study. Agroscope (Switzerland): Annelie Holzkämper (project coordination), Marlies Sommer, Diane Bürge, Patricia Peier and Stephanie Pöschl (laboratory analyses), Dominik Schittli (fieldwork and laboratory analysis), Saïd Elfouki and Hans-Ulrich Zbinden (site management), Severin Neukom (workshop) and the soil quality and soil use group (fieldwork). BOKU (Austria): Kristin Böning, Edberto Moura Lima, Frederike Ding and Sarah Scheiblmair (fieldwork and laboratory analyses), Christine Stumpp (lab management) and the Agricultural School of Hollabrunn for sharing their soil tillage trial. CZU and CARC (Czech Republic): Abdul Majid (laboratory analyses), Eva Kunzová and Mikuláš Madaras (infrastructure). INIA (Spain): Miguel Ángel Porcel and David San Martín (site management and fieldwork), Marta Ribes (fieldwork and laboratory analyses), Paula Béjar and Nazaret Ocaña (fieldwork). SLU (Sweden): Rebecca N. ter Borg, Péter Garamszegi, Wiebke M. Heinze, Jennie Yun (fieldwork) and Anna Eklöv Pettersson (laboratory analyses). Aarhus University (Denmark): Stig T. Rasmussen (fieldwork), Jørgen M. Nielsen (fieldwork and laboratory analyses), Palle Jørgensen (laboratory analyses), Ulla H. Rasmussen (laboratory analyses) and Eugene Driessen (site management and data provider). Open access publishing facilitated by Agroscope, as part of the Wiley - Agroscope agreement via the Consortium Of Swiss Academic Libraries.

Funding

This work was carried out within the framework of the European Joint Programme for SOIL (EJP SOIL), which has received funding from the European Union's Horizon 2020 Research and Innovation Programme under Grant Agreement No. 862695 (SoilX project). Open access funding was provided by Agroscope.

Conflicts of Interest

Prof. Thomas Keller is Associate Editor of *Soil Use and Management* and co-author of this article. He was excluded from editorial decision-making related to the acceptance of this article for publication in the journal. The other authors declare no conflicts of interest.

Data Availability Statement

All data to support this study is publicly available on Zenodo: Full dataset of all 111 plots (Heller, D'Hose, et al. 2024; https://doi.org/10.5281/zenodo.13935388), reduced dataset of 92 plots presented in this study, incl. Code (Heller 2025; https://doi.org/10.5281/zenodo.17434146).

References

Abiven, S., S. Menasseri, and C. Chenu. 2009. "The Effects of Organic Inputs Over Time on Soil Aggregate Stability—A Literature Analysis." *Soil Biology and Biochemistry* 41, no. 1: 1–12. https://doi.org/10.1016/j.soilbio.2008.09.015.

Alakukku, L., P. Weisskopf, W. C. T. Chamen, et al. 2003. "Prevention Strategies for Field Traffic-Induced Subsoil Compaction: A Review: Part 1. Machine/Soil Interactions." *Soil and Tillage Research* 73, no. 1–2: 145–160. https://doi.org/10.1016/S0167-1987(03)00107-7.

Amézketa, E. 1999. "Soil Aggregate Stability: A Review." *Journal of Sustainable Agriculture* 14, no. 2–3: 83–151. https://doi.org/10.1300/J064v14n02_08.

Andriuzzi, W. S., M. M. Pulleman, O. Schmidt, J. H. Faber, and L. Brussaard. 2015. "Anecic Earthworms (*Lumbricus terrestris*) Alleviate Negative Effects of Extreme Rainfall Events on Soil and Plants in Field Mesocosms." *Plant and Soil* 397, no. 1: 103–113. https://doi.org/10.1007/s11104-015-2604-4.

Archer, J. R., and P. D. Smith. 1972. "The Relation Between Bulk Density, Available Water Capacity, and Air Capacity of Soils." *Journal of Soil Science* 23, no. 4: 475–480. https://doi.org/10.1111/j.1365-2389.1972.tb01678.x.

Balesdent, J., I. Basile-Doelsch, J. Chadoeuf, et al. 2017. "Turnover of Deep Organic Carbon in Cultivated Soils: An Estimate From a Review of Isotope Data." *Biotechnology, Agronomy, Society and Environment* 21, no. 3: 181–190. https://doi.org/10.25518/1780-4507.13562.

Barthès, B., and E. Roose. 2002. "Aggregate Stability as an Indicator of Soil Susceptibility to Runoff and Erosion; Validation at Several Levels." *Catena* 47, no. 2: 133–149. https://doi.org/10.1016/S0341-8162(01)00180-1.

Bartoń, K. 2024. "MuMIn: Multi-Model Inference." R Package Version 1.48.4. https://doi.org/10.32614/CRAN.package.MuMIn.

Basset, C., M. Abou Najm, T. Ghezzehei, X. Hao, and A. Daccache. 2023. "How Does Soil Structure Affect Water Infiltration? A Meta-Data Systematic Review." *Soil and Tillage Research* 226: 105577. https://doi.org/10.1016/j.still.2022.105577.

Bates, D., M. Maechler, B. Bolker, and S. Walker. 2015. "Fitting Linear Mixed-Effects Models Using lme4." *Journal of Statistical Software* 67, no. 1: 1–48. https://doi.org/10.18637/jss.v067.i01.

Bengough, A. G., B. M. McKenzie, P. D. Hallett, and T. A. Valentine. 2011. "Root Elongation, Water Stress, and Mechanical Impedance: A Review of Limiting Stresses and Beneficial Root Tip Traits." *Journal of Experimental Botany* 62, no. 1: 59–68. https://doi.org/10.1093/jxb/erq350.

Blanchy, G., L. Albrecht, G. Bragato, S. Garré, N. Jarvis, and J. Koestel. 2023. "Impacts of Soil Management and Climate on Saturated and Near-Saturated Hydraulic Conductivity: Analyses of the Open Tension-Disk Infiltrometer Meta-Database (OTIM)." *Hydrology and Earth System Sciences* 27, no. 14: 2703–2724. https://doi.org/10.5194/hess-27-2703-2023.

Blanchy, G., G. Bragato, C. Di Bene, et al. 2023. "Soil and Crop Management Practices and the Water Regulation Functions of Soils: A Qualitative Synthesis of Meta-Analyses Relevant to European Agriculture." *Soil* 9, no. 1: 1–20. https://doi.org/10.5194/soil-9-1-2023.

Blanco-Canqui, H., and S. J. Ruis. 2018. "No-Tillage and Soil Physical Environment." *Geoderma* 326: 164–200. https://doi.org/10.1016/j.geoderma.2018.03.011.

Blanco-Canqui, H., C. A. Shapiro, C. S. Wortmann, et al. 2013. "Soil Organic Carbon: The Value to Soil Properties." *Journal of Soil and Water Conservation* 68, no. 5: 129A–134A. https://doi.org/10.2489/jswc.68.5.129A.

Blouin, M., M. E. Hodson, E. A. Delgado, et al. 2013. "A Review of Earthworm Impact on Soil Function and Ecosystem Services." *European Journal of Soil Science* 64, no. 2: 161–182. https://doi.org/10.1111/ejss.12025.

Bodner, G., A. Nakhforoosh, and H. P. Kaul. 2015. "Management of Crop Water Under Drought: A Review." *Agronomy for Sustainable Development* 35, no. 2: 401–442. https://doi.org/10.1007/s13593-015-0283-4.

Briones, M., and O. Schmidt. 2017. "Conventional Tillage Decreases the Abundance and Biomass of Earthworms and Alters Their Community Structure in a Global Meta-Analysis." *Global Change Biology* 23: 4396–4419. https://doi.org/10.1111/gcb.13744.

Butt, K. R., and N. Grigoropoulou. 2010. "Basic Research Tools for Earthworm Ecology." *Applied and Environmental Soil Science* 2010, no. 1: 562816. https://doi.org/10.1155/2010/562816.

Capowiez, Y., S. Cadoux, P. Bouchant, et al. 2009. "The Effect of Tillage Type and Cropping System on Earthworm Communities, Macroporosity and Water Infiltration." *Soil and Tillage Research* 105, no. 2: 209–216. https://doi.org/10.1016/j.still.2009.09.002.

Capowiez, Y., D. Marchán, T. Decaëns, M. Hedde, and N. Bottinelli. 2024. "Let Earthworms Be Functional-Definition of New Functional Groups Based on Their Bioturbation Behavior." *Soil Biology and Biochemistry* 188: 109209. https://doi.org/10.1016/j.soilbio.2023.109209.

Cardinael, R., B. Guenet, T. Chevallier, C. Dupraz, T. Cozzi, and C. Chenu. 2018. "High Organic Inputs Explain Shallow and Deep SOC Storage in a Long-Term Agroforestry System–Combining Experimental and Modeling Approaches." *Biogeosciences* 15, no. 1: 297–317. https://doi.org/10.5194/bg-15-297-2018.

Chamen, T., L. Alakukku, S. Pires, et al. 2003. "Prevention Strategies for Field Traffic-Induced Subsoil Compaction: A Review: Part 2. Equipment and Field Practices." *Soil and Tillage Research* 73, no. 1–2: 161–174. https://doi.org/10.1016/S0167-1987(03)00108-9.

Cotrufo, M. F., and J. M. Lavallee. 2022. "Soil Organic Matter Formation, Persistence, and Functioning: A Synthesis of Current Understanding to Inform Its Conservation and Regeneration." *Advances in Agronomy* 172: 1–66. https://doi.org/10.1016/bs.agron.2021.11.002.

Davidson, E. A., and I. A. Janssens. 2006. "Temperature Sensitivity of Soil Carbon Decomposition and Feedbacks to Climate Change." *Nature* 440, no. 7081: 165–173. https://doi.org/10.1038/nature04514.

Dettmann, U. 2023. "SoilHyP: Soil Hydraulic Properties." R Package Version 0.1.7. https://doi.org/10.32614/CRAN.package.SoilHyP.

Dexter, A. R., E. A. Czyż, and O. P. Gaţe. 2007. "A Method for Prediction of Soil Penetration Resistance." *Soil and Tillage Research* 93, no. 2: 412–419. https://doi.org/10.1016/j.still.2006.05.011.

D'Hose, T., G. Ruysschaert, N. Viaene, et al. 2016. "Farm Compost Amendment and Non-Inversion Tillage Improve Soil Quality Without Increasing the Risk for N and P Leaching." *Agriculture, Ecosystems & Environment* 225: 126–139. https://doi.org/10.1016/j.agee.2016.03.035.

Dungait, J. A., D. W. Hopkins, A. S. Gregory, and A. P. Whitmore. 2012. "Soil Organic Matter Turnover Is Governed by Accessibility Not Recalcitrance." *Global Change Biology* 18, no. 6: 1781–1796. https://doi.org/10.1111/j.1365-2486.2012.02665.x.

Edlinger, A., G. Garland, S. Banerjee, et al. 2023. "The Impact of Agricultural Management on Soil Aggregation and Carbon Storage Is Regulated by Climatic Thresholds Across a 3000 Km European Gradient." *Global Change Biology* 29, no. 11: 3177–3192. https://doi.org/10.1111/gcb.16677.

Eisenhauer, N., M. A. Bowker, J. B. Grace, and J. R. Powell. 2015. "From Patterns to Causal Understanding: Structural Equation Modeling (SEM) in Soil Ecology." *Pedobiologia* 58, no. 2–3: 65–72. https://doi.org/10.1016/j.pedobi.2015.03.002.

Fox, J., and G. Monette. 1992. "Generalized Collinearity Diagnostics." *Journal of the American Statistical Association* 87, no. 417: 178–183. https://doi.org/10.1080/01621459.1992.10475190.

Francis, G. S., and P. M. Fraser. 1998. "The Effects of Three Earthworm Species on Soil Macroporosity and Hydraulic Conductivity." *Applied Soil Ecology* 10, no. 1–2: 11–19. https://doi.org/10.1016/S0929-1393(98)00045-6.

Garland, G., A. Edlinger, S. Banerjee, et al. 2021. "Crop Cover Is More Important Than Rotational Diversity for Soil Multifunctionality and Cereal Yields in European Cropping Systems." *Nature Food* 2, no. 1: 28–37.

Geers-Lucas, M., M. Leue, S. Schlüter, and M. Sommer. 2025. "Long-Term Improvement of Subsoil Pore Structure in Sandy Soils by Meliorative Fractional Deep Tillage." *Geoderma* 463: 117556. https://doi.org/10.1016/j.geoderma.2025.117556.

Gómez-Muñoz, B., L. S. Jensen, L. Munkholm, J. E. Olesen, E. Møller Hansen, and S. Bruun. 2021. "Long-Term Effect of Tillage and Straw Retention in Conservation Agriculture Systems on Soil Carbon Storage." *Soil Science Society of America Journal* 85, no. 5: 1465–1478. https://doi.org/10.1002/saj2.2031.

Grace, J. B. 2006. *Structural Equation Modeling and Natural Systems*, 378. Cambridge University Press.

Groemping, U. 2007. "Relative Importance for Linear Regression in R: The Package Relaimpo." *Journal of Statistical Software* 17, no. 1: 1–27. https://doi.org/10.18637/jss.v017.i01.

Gubler, A., D. Wächter, and P. Schwab. 2018. "Homogenisation of Series of Soil Organic Carbon: Harmonising Results by Wet Oxidation (Swiss Standard Method) and Dry Combustion." *Agroscope Science* 62: 1–9. https://ira.agroscope.ch/en-US/publication/37689.

Guimarães, R. M., M. Lamandé, L. J. Munkholm, B. C. Ball, and T. Keller. 2017. "Opportunities and Future Directions for Visual Soil Evaluation Methods in Soil Structure Research." *Soil and Tillage Research* 173: 104–113. https://doi.org/10.1016/j.still.2017.01.016.

Guimarães, R. M. L., B. C. Ball, and C. A. Tormena. 2011. "Improvements in the Visual Evaluation of Soil Structure." *Soil Use and Management* 27, no. 3: 395–403. https://doi.org/10.1111/j.1475-2743.2011.00354.x.

Hartley, I. P., T. C. Hill, S. E. Chadburn, and G. Hugelius. 2021. "Temperature Effects on Carbon Storage Are Controlled by Soil Stabilisation Capacities." *Nature Communications* 12, no. 1: 6713. https://doi.org/10.1038/s41467-021-27101-1.

Heinemann, H., J. Hirte, F. Seidel, and A. Don. 2023. "Increasing Root Biomass Derived Carbon Input to Agricultural Soils by Genotype Selection—A Review." *Plant and Soil* 490, no. 1: 19–30. https://doi.org/10.1007/s11104-023-06068-6.

Heitman, J. L., D. Kool, and H. D. Carvalho. 2023. "Soil Management Considerations for Water Resiliency in a Changing Climate." *Agronomy Journal* 115, no. 5: 2127–2139. https://doi.org/10.1002/agj2.21425.

Heller, O. 2025. "Data to Support 'Carbon Input and Tillage Intensity Modulate Pedo-Climatic Controls of Topsoil but Not Subsoil Physical Properties' [Data Set]." *Zenodo*. https://doi.org/10.5281/zenodo.17434145.

Heller, O., A. Chervet, F. Durand-Maniclas, et al. 2025. "SoilManageR—An R Package for Deriving Soil Management Indicators to Harmonize Agricultural Practice Assessments." *European Journal of Soil Science* 76: e70102. https://doi.org/10.1111/ejss.70102.

Heller, O., T. D'Hose, P. Euteneuer, et al. 2024. "SoilX Sampling and Measurements Protocol, WP2 2023." *Zenodo*. https://doi.org/10.5281/zenodo.14008500.

Heller, O., L. ten Damme, T. D'Hose, et al. 2024. "SoilX D2.2: Dataset of Physical, Biological and Chemical Soil Properties From 10 European Long-Term Experiments (Version 1) [Data Set]." *Zenodo*. https://doi.org/10.5281/zenodo.13935388.

Hernanz, J. L., H. Peixoto, C. Cerisola, and V. Sánchez-Girón. 2000. "An Empirical Model to Predict Soil Bulk Density Profiles in Field Conditions Using Penetration Resistance, Moisture Content and Soil Depth." *Journal of Terramechanics* 37, no. 4: 167–184. https://doi.org/10.1016/S0022-4898(99)00020-8.

Hlisnikovský, L., L. Menšík, and E. Kunzová. 2020. "The Development of Winter Wheat Yield and Quality Under Different Fertilizer Regimes and Soil-Climatic Conditions in The Czech Republic." *Agronomy* 10, no. 8: 1160. https://doi.org/10.3390/agronomy10081160.

Holz, D. J., K. W. Williard, P. J. Edwards, and J. E. Schoonover. 2015. "Soil Erosion in Humid Regions: A Review." *Journal of Contemporary Water Research & Education* 154, no. 1: 48–59. https://doi.org/10.1111/j.1936-704X.2015.03187.x.

Holzkämper, A., L. ten Damme, T. D'Hose, et al. 2024. "EJPSOIL-SoilX: Final Project Report." *Zenodo*. https://doi.org/10.5281/zenodo.14001120.

Jarvis, N., J. Forkman, J. Koestel, T. Kätterer, M. Larsbo, and A. Taylor. 2017. "Long-Term Effects of Grass-Clover Leys on the Structure of a Silt Loam Soil in a Cold Climate." *Agriculture, Ecosystems & Environment* 247: 319–328. https://doi.org/10.1016/j.agee.2017.06.042.

Jarvis, N., J. Koestel, I. Messing, J. Moeys, and A. Lindahl. 2013. "Influence of Soil, Land Use and Climatic Factors on the Hydraulic Conductivity of Soil." *Hydrology and Earth System Sciences* 17, no. 12: 5185–5195. https://doi.org/10.5194/hess-17-5185-2013.

Jarvis, N., and M. Larsbo. 2023. "Macropores and Macropore Flow." *Encyclopedia of Soils in the Environment (Second Edition)* 5: 306–313. https://doi.org/10.1016/B978-0-12-822974-3.00098-7.

Jarvis, N. J. 2007. "A Review of Non-Equilibrium Water Flow and Solute Transport in Soil Macropores: Principles, Controlling Factors and Consequences for Water Quality." *European Journal of Soil Science* 58, no. 3: 523–546. https://doi.org/10.1111/j.1365-2389.2007.00915.x.

JRC. n.d. "AGRI4CAST Resources Portal. European Commission, Joint Research Centre (JRC), Ispra (Italy)." https://agri4cast.jrc.ec.europa.eu/dataportal.

Kautz, T. 2015. "Research on Subsoil Biopores and Their Functions in Organically Managed Soils: A Review." *Renewable Agriculture and Food Systems* 30, no. 4: 318–327. https://doi.org/10.1017/S1742170513000549.

Kay, B. D., and D. A. Angers. 2001. "Soil Structure." In *Soil Physics Companion*, edited by A. W. Warrick, 1th ed., 249–295. CRC Press.

Keller, T., M. Sandin, T. Colombi, R. Horn, and D. Or. 2019. "Historical Increase in Agricultural Machinery Weights Enhanced Soil Stress Levels and Adversely Affected Soil Functioning." *Soil and Tillage Research* 194: 104293. https://doi.org/10.1016/j.still.2019.104293.

Kirschbaum, M. U. 1995. "The Temperature Dependence of Soil Organic Matter Decomposition, and the Effect of Global Warming on Soil Organic C Storage." *Soil Biology and Biochemistry* 27, no. 6: 753–760. https://doi.org/10.1016/0038-0717(94)00242-S.

Klöffel, T., J. Barron, A. Nemes, D. Giménez, and N. Jarvis. 2024. "Soil, Climate, Ti Me and Site Factors as Drivers of Soil Structure Evolution in Agricultural Soils From a Temperate-Boreal Region." *Geoderma* 442: 116772. https://doi.org/10.1016/j.geoderma.2024.116772.

Kuznetsova, A., P. B. Brockhoff, and R. H. B. Christensen. 2017. "lmerTest Package: Tests in Linear Mixed Effects Models." *Journal of Statistical Software* 82, no. 13: 1–26. https://doi.org/10.18637/jss.v082.i13.

Kuzyakov, Y., and Y. Kooch. 2024. "Earthworm Biopores for Transport and Nutrient Cycling." In *Earthworms and Ecological Processes*, 417–432. Springer. https://doi.org/10.1007/978-3-031-64510-5_16.

Lai, J., W. Zhu, D. Cui, and L. Mao. 2023. "Extension of the Glmm. Hp Package to Zero-Inflated Generalized Linear Mixed Models and Multiple Regression." *Journal of Plant Ecology* 16, no. 6: rtad038. https://doi.org/10.1093/jpe/rtad038.

Lal, R. 2020. "Soil Organic Matter and Water Retention." *Agronomy Journal* 112, no. 5: 3265–3277. https://doi.org/10.1002/agj2.20282.

Lefcheck, J. S. 2016. "piecewiseSEM: Piecewise Structural Equation Modelling in r for Ecology, Evolution, and Systematics." *Methods in Ecology and Evolution* 7, no. 5: 573–579. https://doi.org/10.1111/2041-210X.12512.

Libohova, Z., C. Seybold, D. Wysocki, et al. 2018. "Reevaluating the Effects of Soil Organic Matter and Other Properties on Available Water-Holding Capacity Using the National Cooperative Soil Survey Characterization Database." *Journal of Soil and Water Conservation* 73, no. 4: 411–421. https://doi.org/10.2489/jswc.73.4.411.

Liu, C., X. Zhang, and Y. Zhang. 2002. "Determination of Daily Evaporation and Evapotranspiration of Winter Wheat and Maize by Large-Scale Weighing Lysimeter and Micro-Lysimeter." *Agricultural and Forest Meteorology* 111, no. 2: 109–120. https://doi.org/10.1016/S0168-1923(02)00015-1.

Lorenz, K., and R. Lal. 2005. "The Depth Distribution of Soil Organic Carbon in Relation to Land Use and Management and the Potential of Carbon Sequestration in Subsoil Horizons." *Advances in Agronomy* 88: 35–66. https://doi.org/10.1016/S0065-2113(05)88002-2.

Lucas, M., S. Schlüter, H. J. Vogel, and D. Vetterlein. 2019. "Soil Structure Formation Along an Agricultural Chronosequence." *Geoderma* 350: 61–72. https://doi.org/10.1016/j.geoderma.2019.04.041.

Maltas, A., H. Kebli, H. R. Oberholzer, P. Weisskopf, and S. Sinaj. 2018. "The Effects of Organic and Mineral Fertilizers on Carbon Sequestration, Soil Properties, and Crop Yields From a Long-Term Field Experiment Under a Swiss Conventional Farming System." *Land Degradation & Development* 29, no. 4: 926–938. https://doi.org/10.1002/ldr.2913.

Martin-Rueda, I., L. M. Munoz-Guerra, F. Yunta, E. Esteban, J. L. Tenorio, and J. J. Lucena. 2007. "Tillage and Crop Rotation Effects on Barley Yield and Soil Nutrients on a Calciortidic Haploxeralf." *Soil and Tillage Research* 92, no. 1–2: 1–9. https://doi.org/10.1016/j.still.2005.10.006.

McBeath, T., S. Davies, and J. Kirkegaard. 2026. "Never Say Never: The Interdependence of No-Till and Strategic Deep Tillage in Sustainable Production Systems." *Crop and Environment* 5, no. 3: 100130. https://doi.org/10.1016/j.crope.2026.100130.

McCallum, M. H., J. A. Kirkegaard, T. W. Green, et al. 2004. "Improved Subsoil Macroporosity Following Perennial Pastures." *Australian Journal of Experimental Agriculture* 44, no. 3: 299–307. https://doi.org/10.1071/EA03076.

Minasny, B., and A. B. McBratney. 2018. "Limited Effect of Organic Matter on Soil Available Water Capacity." *European Journal of Soil Science* 69, no. 1: 39–47.

Miner, G. L., J. A. Delgado, J. A. Ippolito, and C. E. Stewart. 2020. "Soil Health Management Practices and Crop Productivity." *Agricultural & Environmental Letters* 5, no. 1: e20023. https://doi.org/10.1002/ael2.20023.

Moeys, J. 2024. "soiltexture: Functions for Soil Texture Plot, Classification and Transformation." R Package Version 1.5.3. https://doi.org/10.32614/CRAN.package.soiltexture.

Moraes, M. T. D., H. Debiasi, R. Carlesso, J. C. Franchini, and V. R. D. Silva. 2014. "Critical Limits of Soil Penetration Resistance in a Rhodic Eutrudox." *Revista Brasileira de Ciência do Solo* 38: 288–298. https://doi.org/10.1590/S0100-06832014000100029.

Nemes, A., W. J. Rawls, and Y. A. Pachepsky. 2005. "Influence of Organic Matter on the Estimation of Saturated Hydraulic Conductivity." *Soil Science Society of America Journal* 69, no. 4: 1330–1337. https://doi.org/10.2136/sssaj2004.0055.

Nemes, A., J. H. M. Wösten, A. Lilly, and J. O. Voshaar. 1999. "Evaluation of Different Procedures to Interpolate Particle-Size Distributions to Achieve Compatibility Within Soil Databases." *Geoderma* 90, no. 3–4: 187–202. https://doi.org/10.1016/S0016-7061(99)00014-2.

Nimmo, J. R., and K. S. Perkins. 2002. "2.6 Aggregate Stability and Size Distribution." *Methods of Soil Analysis: Part 4 Physical Methods* 5: 317–328. https://doi.org/10.2136/sssabookser5.4.c14.

Nyaupane, K., U. Mishra, F. Tao, et al. 2024. "Observational Benchmarks Inform Representation of Soil Organic Carbon Dynamics in Land Surface Models." *Biogeosciences* 21, no. 22: 5173–5183. https://doi.org/10.5194/bg-21-5173-2024.

Oberholzer, H. R., J. Leifeld, and J. Mayer. 2014. "Changes in Soil Carbon and Crop Yield Over 60 Years in the Zurich Organic Fertilization Experiment, Following Land-Use Change From Grassland to Cropland." *Journal of Plant Nutrition and Soil Science* 177, no. 5: 696–704. https://doi.org/10.1002/jpln.201300385.

Olsen, H. J. 1988. "Technology Showcase Electronic Penetrometer for Field Tests." *Journal of Terramechanics* 25, no. 4: 287–293. https://doi.org/10.1016/0022-4898(88)90042-0.

Pachepsky, Y., and W. J. Rawls, eds. 2004. "Development of Pedotransfer Functions in Soil Hydrology." In *Developments in Soil Science*, vol. 30. Elsevier.

Palm, C., H. Blanco-Canqui, F. DeClerck, L. Gatere, and P. Grace. 2014. "Conservation Agriculture and Ecosystem Services: An Overview." *Agriculture, Ecosystems & Environment* 187: 87–105. https://doi.org/10.1016/j.agee.2013.10.010.

Phillips, H. R. P., C. A. Guerra, M. L. C. Bartz, et al. 2019. "Global Distribution of Earthworm Diversity." *Science* 366: 480–485. https://doi.org/10.1126/science.aax4851.

Poffenbarger, H. J., D. W. Barker, M. J. Helmers, et al. 2017. "Maximum Soil Organic Carbon Storage in Midwest US Cropping Systems When Crops Are Optimally Nitrogen-Fertilized." *PLoS One* 12, no. 3: e0172293. https://doi.org/10.1371/journal.pone.0172293.

Pribyl, D. W. 2010. "A Critical Review of the Conventional SOC to SOM Conversion Factor." *Geoderma* 156, no. 3–4: 75–83. https://doi.org/10.1016/j.geoderma.2010.02.003.

R Core Team. 2024. *R: A Language and Environment for Statistical Computing*. R Foundation for Statistical Computing. https://www.R-project.org/.

Rabot, E., M. Wiesmeier, S. Schlüter, and H. J. Vogel. 2018. "Soil Structure as an Indicator of Soil Functions: A Review." *Geoderma* 314: 122–137. https://doi.org/10.1016/j.geoderma.2017.11.009.

Ramos, T. B., H. Darouich, and L. S. Pereira. 2024. "Mulching Effects on Soil Evaporation, Crop Evapotranspiration and Crop Coefficients: A Review Aimed at Improved Irrigation Management." *Irrigation Science* 42, no. 3: 525–539. https://doi.org/10.1007/s00271-024-00924-8.

Roel-Rezk, V., W. R. Horwath, and C. M. Pittelkow. 2025. "Is Soil Health Research Meeting Its Potential? Analysis of Studies in California and Implications for Ecosystem Services." *Soil Science Society of America Journal* 89, no. 5: e70139. https://doi.org/10.1002/saj2.70139.

Rosner, K., G. Bodner, K. Hage-Ahmed, and S. Steinkellner. 2018. "Long-Term Soil Tillage and Cover Cropping Affected Arbuscular Mycorrhizal Fungi, Nutrient Concentrations, and Yield in Sunflower." *Agronomy Journal* 110, no. 6: 2664–2672.

Saco, P. M., K. R. McDonough, J. F. Rodriguez, J. Rivera-Zayas, and S. G. Sandi. 2021. "The Role of Soils in the Regulation of Hazards and Extreme Events." *Philosophical Transactions of the Royal Society B* 376, no. 1834: 20200178. https://doi.org/10.1098/rstb.2020.0178.

Sánchez-Moreno, S., M. B. Ros, F. Walder, et al. 2025. "A Global Dataset of Experimental Agricultural Management on Soil Carbon Accrual, Its Synergies and Trade-Offs." *Scientific Data* 12, no. 1: 929. https://doi.org/10.1038/s41597-025-05238-8.

Sarkar, S., K. Germer, R. Maity, and W. Durner. 2019a. "Measuring Near-Saturated Hydraulic Conductivity of Soils by Quasi Unit-Gradient Percolation—1. Theory and Numerical Analysis." *Journal of Plant Nutrition and Soil Science* 182: 524–534. https://doi.org/10.1002/jpln.201800382.

Sarkar, S., K. Germer, R. Maity, and W. Durner. 2019b. "Measuring Near-Saturated Hydraulic Conductivity of Soils by Quasi Unit-Gradient Percolation—2. Application of the Methodology." *Journal of Plant Nutrition and Soil Science* 182: 535–540. https://doi.org/10.1002/jpln.201800383.

Schjønning, P., R. A. McBride, T. Keller, and P. B. Obour. 2017. "Predicting Soil Particle Density From Clay and Soil Organic Matter Contents." *Geoderma* 286: 83–87. https://doi.org/10.1016/j.geoderma.2016.10.020.

Schlüter, S., L. Albrecht, K. Schwärzel, and J. Kreiselmeier. 2020. "Long-Term Effects of Conventional Tillage and No-Tillage on Saturated and Near-Saturated Hydraulic Conductivity—Can Their Prediction Be Improved by Pore Metrics Obtained With X-Ray CT?" *Geoderma* 361: 114082. https://doi.org/10.1016/j.geoderma.2019.114082.

Schlüter, S., U. Weller, and H. J. Vogel. 2011. "Soil-Structure Development Including Seasonal Dynamics in a Long-Term Fertilization Experiment." *Journal of Plant Nutrition and Soil Science* 174, no. 3: 395–403. https://doi.org/10.1002/jpln.201000103.

Schneider, F., A. Don, I. Hennings, O. Schmittmann, and S. J. Seidel. 2017. "The Effect of Deep Tillage on Crop Yield–What Do We Really Know?" *Soil and Tillage Research* 174: 193–204. https://doi.org/10.1016/j.still.2017.07.005.

Seitz, S., P. Goebes, V. L. Puerta, et al. 2019. "Conservation Tillage and Organic Farming Reduce Soil Erosion." *Agronomy for Sustainable Development* 39, no. 1: 4. https://doi.org/10.1007/s13593-018-0545-z.

Seybold, C. A., and D. S. Harms. 2012. "Estimation of −1500 kPa Water Retention in Soil Survey." *Soil Science* 177, no. 4: 229–235. https://doi.org/10.1097/SS.0b013e31824826af.

Shipley, B. 2009. "Confirmatory Path Analysis in a Generalized Multilevel Context." *Ecology* 90, no. 2: 363–368. https://doi.org/10.1890/08-1034.1.

Simon, B., I. Dekemati, H. T. M. Ibrahim, et al. 2025. "Impact of Tillage Practices and Soil Texture on Soil Health and Earthworms in the Pannonian Region: A Comparative Study From Austria and Hungary." *Applied Soil Ecology* 206: 105863. https://doi.org/10.1016/j.apsoil.2025.105863.

Six, J., H. Bossuyt, S. Degryze, and K. Denef. 2004. "A History of Research on the Link Between (Micro) Aggregates, Soil Biota, and Soil Organic Matter Dynamics." *Soil and Tillage Research* 79, no. 1: 7–31. https://doi.org/10.1016/j.still.2004.03.008.

Smith, L. C., A. Orgiazzi, N. Eisenhauer, et al. 2021. "Large-Scale Drivers of Relationships Between Soil Microbial Properties and Organic Carbon Across Europe." *Global Ecology and Biogeography* 30, no. 10: 2070–2083. https://doi.org/10.1111/geb.13371.

Soil Science Division Staff. 2017. "Soil Survey Manual." In *USDA Handbook 18*, edited by C. Ditzler, K. Scheffe, and H. C. Monger. Government Printing Office. https://www.nrcs.usda.gov/resources/guides-and-instructions/soil-survey-manual.

Stepniewski, W., J. Gliński, and B. C. Ball. 1994. "Effects of Compaction on Soil Aeration Properties." In *Developments in Agricultural Engineering*, vol. 11, 167–189. Elsevier. https://doi.org/10.1016/B978-0-444-88286-8.50016-7.

Strudley, M. W., T. R. Green, and J. C. Ascough II. 2008. "Tillage Effects on Soil Hydraulic Properties in Space and Time: State of the Science." *Soil and Tillage Research* 99, no. 1: 4–48. https://doi.org/10.1016/j.still.2008.01.007.

Sturm, L., H. Wagentristl, R. W. Neugschwandtner, et al. 2026. "Earthworms Are Sustained in a 116-Year Rye Monoculture With Ploughing by Provision of Soil Organic Carbon From Farmyard Manure." *European Journal of Soil Biology* 128: 103815. https://doi.org/10.1016/j.ejsobi.2026.103815.

Sun, W., J. G. Canadell, L. Yu, et al. 2020. "Climate Drives Global Soil Carbon Sequestration and Crop Yield Changes Under Conservation Agriculture." *Global Change Biology* 26, no. 6: 3325–3335. https://doi.org/10.1111/gcb.15001.

Szabó, B., M. Weynants, and T. K. Weber. 2021. "Updated European Hydraulic Pedotransfer Functions With Communicated Uncertainties in the Predicted Variables (euptfv2)." *Geoscientific Model Development* 14, no. 1: 151–175. https://doi.org/10.5194/gmd-14-151-2021.

Tang, S., W. Pan, Y. Yang, et al. 2025. "Soil Carbon Sequestration Enhanced by Long-Term Nitrogen and Phosphorus Fertilization." *Nature Geoscience* 18, no. 10: 1005–1013. https://doi.org/10.1038/s41561-025-01789-y.

ten Damme, L., M. Goberna, S. Sánchez-Moreno, et al. 2025. "Long-Term Application of No-Tillage-Induced Greater Risk of Poor Topsoil Aeration

Along a European Pedoclimatic Gradient." *European Journal of Soil Science* 76, no. 2: e70081. https://doi.org/10.1111/ejss.70081.

ten Damme, L., P. Schjønning, L. J. Munkholm, O. Green, S. K. Nielsen, and M. Lamandé. 2021. "Soil Structure Response to Field Traffic: Effects of Traction and Repeated Wheeling." *Soil and Tillage Research* 213: 105128. https://doi.org/10.1016/j.still.2021.105128.

Thorsøe, M. H., S. Keesstra, M. De Boever, et al. 2023. "Sustainable Soil Management: Soil Knowledge Use and Gaps in Europe." *European Journal of Soil Science* 74, no. 6: e13439. https://doi.org/10.1111/ejss.13439.

Torppa, K. A., and A. R. Taylor. 2022. "Alternative Combinations of Tillage Practices and Crop Rotations Can Foster Earthworm Density and Bioturbation." *Applied Soil Ecology* 175: 104460. https://doi.org/10.1016/j.apsoil.2022.104460.

Weber, T. K. D., L. Weihermüller, A. Nemes, et al. 2024. "Hydro-Pedotransfer Functions: A Roadmap for Future Development." *Hydrology and Earth System Sciences* 28, no. 14: 3391–3433. https://doi.org/10.5194/hess-28-3391-2024.

Wiesmeier, M., L. Urbanski, E. Hobley, et al. 2019. "Soil Organic Carbon Storage as a Key Function of Soils-A Review of Drivers and Indicators at Various Scales." *Geoderma* 333: 149–162. https://doi.org/10.1016/j.geoderma.2018.07.026.

Wittwer, R. A., S. F. Bender, K. Hartman, et al. 2021. "Organic and Conservation Agriculture Promote Ecosystem Multifunctionality." *Science Advances* 7, no. 34: eabg6995. https://doi.org/10.1126/sciadv.abg6995.

Yost, J. L., and A. E. Hartemink. 2020. "How Deep Is the Soil Studied—An Analysis of Four Soil Science Journals." *Plant and Soil* 452, no. 1: 5–18. https://doi.org/10.1007/s11104-020-04550-z.

Zhang, Y., and M. G. Schaap. 2017. "Weighted Recalibration of the Rosetta Pedotransfer Model With Improved Estimates of Hydraulic Parameter Distributions and Summary Statistics (Rosetta3)." *Journal of Hydrology* 547: 39–53. https://doi.org/10.1016/j.jhydrol.2017.01.004.

Supporting Information

Additional supporting information can be found online in the Supporting Information section. **Appendix S1:** sum70247-sup-0001-Supinfo.docx. **Figure S1:** Pearson's correlation coefficients r of pairwise correlations of soil physical properties. $N = 184$. Abbreviations refer to soil organic carbon content (SOC), bulk density (BD), gravimetric plant available water (PAW), volumetric air capacity (AC), $\log_{10}$-transformed hydraulic conductivity of the soil matrix (K_{5hPa}) and the macropores (K_{sat}), field penetration resistance (FPR) and water stable aggregate index (WSA). **Figure S2:** Piecewise structural equation model (pSEM) showing direct and indirect effects on plant available water (PAW) in the topsoil. For details, see the legend of Figure 6 in the main text. **Figure S3:** Piecewise structural equation model (pSEM) showing direct and indirect effects on plant available water (PAW) in the subsoil. For details, see the legend of Figure 6 in the main text. **Figure S4:** Piecewise structural equation model (pSEM) showing direct and indirect effects on air capacity (AC) in the topsoil. For details, see the legend of Figure 6 in the main text. **Figure S5:** Piecewise structural equation model (pSEM) showing direct and indirect effects on air capacity at −100 hPa matric potential (AC) in the subsoil. For details, see the legend of Figure 6 in the main text. **Figure S6:** Piecewise structural equation model (pSEM) showing direct and indirect effects on the matrix conductivity (K_{5hPa}) in the topsoil. For details, see the legend of Figure 6 in the main text. **Figure S7:** Piecewise structural equation model (pSEM) showing direct and indirect effects on matrix conductivity (K_{5hPa}) in the subsoil. For details, see the legend of Figure 6 in the main text. **Figure S8:** Piecewise structural equation model (pSEM) showing direct and indirect effects on saturated conductivity (K_{sat}) in the topsoil. For details, see the legend of Figure 6 in the main text. **Figure S9:** Piecewise structural equation model (pSEM) showing direct and indirect effects on saturated conductivity (K_{sat}) in the subsoil. For details, see the legend of Figure 6 in the main text. **Figure S10:** Piecewise structural equation model (pSEM) showing direct and indirect effects on field penetration resistance (FPR) of the core sample sampling interval in the topsoil (see Figure 3 in the main text). For details, see the legend of Figure 6 in the main text. **Figure S11:** Piecewise structural equation model (pSEM) showing direct and indirect effects on field penetration resistance (FPR) of the core sample sampling interval in the subsoil (see Figure 3 in the main text). For details, see the legend of Figure 6 in the main text. **Figure S12:** Piecewise structural equation model (pSEM) showing direct and indirect effects on water stable aggregate index (WSA) in the topsoil. For details, see the legend of Figure 6 in the main text. **Figure S13:** Piecewise structural equation model (pSEM) showing direct and indirect effects on water stable aggregate index (WSA) in the subsoil. For details, see the legend of Figure 6 in the main text. **Figure S14:** Piecewise structural equation model (pSEM) showing direct and indirect effects on the visual evaluation of soil structure score (VESS score). VESS scores were inverted (higher VESS score value = better). For details, see the legend of Figure 6 in the main text. **Figure S15:** Relative importance of the predictor variables of the final linear model to explain the soil physical properties with other soil properties. The relative importance shown in Table 2 are multiplied with the adjusted R^2 to calculate the share of the total variability that is explained by the respective explanatory variable. Variables without a bar were either omitted from the initial model in backward variable selection (see main text) or were not included in the initial model. 'Small cores' is a Boolean variable that was one if weather 100 cm^3 soil cores were used and zero otherwise. Colours indicate the paradigm of the effect—blue is a positive effect, red a negative effect. For the analysis the VESS score was inverted (higher value means better score). AC, air capacity; BD, Bulk density; FPR, field penetration resistance; K, hydraulic conductivities; PAW, plant available water; SOC, soil organic carbon; WSA, Water stable aggregate index. Significance level of the effect: p-value $= 0.1 \geq \cdot > 0.05 \geq {*} > 0.01 \geq {**} > 0.001 \geq {***}$. **Figure S16:** Relative importance of the predictor variables of the final mixed-effect models to explain earthworm abundance and scores of the visual soil evaluation (VESS) with pedo-climatic context and management intensities. The relative importance refers to the share of the total variability that is explained by the respective explanatory variable. Variables without a bar were either omitted from the initial model in backward variable selection (see main text) or were not included in the initial model. Colours indicate the paradigm of the effect—blue is a positive effect, red a negative effect. For the analysis the VESS score was inverted (higher value means better score). BD, bulk density; MAP, mean annual precipitation sum; MAT, mean annual temperature; STIR, soil tillage intensity rating. Significance level of the effect: p-value $= 0.1 \geq \cdot > 0.05 \geq {*} > 0.01 \geq {**} > 0.001 \geq {***}$. **Figure S17:** Relative importance of the predictor variables (labels on the left side) of the final mixed-effect models to explain topsoil and subsoil SOC, BD and physical properties (labels on the right side). The relative importance refers to the share of the total variability that is explained by the respective explanatory variable. Variables without a bar were either omitted from the initial model in backward variable selection (see main text) or were not included in the initial model. Colours indicate the paradigm of the effect—blue is a positive effect, red a negative effect. AC, air capacity; BD, bulk density; FPR, field penetration resistance; K, hydraulic conductivities; MAP, mean annual precipitation sum; MAT, mean annual temperature; PAW, plant available water; SOC, soil organic carbon; STIR, soil tillage intensity rating; WSA, Water stable aggregate index. Significance level of the effect: p-value $= 0.1 \geq \cdot > 0.05 \geq {*} > 0.01 \geq {**} > 0.001 \geq {***}$. **Figure S18:** Topsoil volumetric water content at sampling. The dashed vertical dashed lines indicate the depth- and LTE-specific median volumetric water content at permanent wilting point (PWP, −15,000 hPa) and at field capacity (FC, −100 hPa) as well the median porosity. Abbreviations of LTEs are the same as in Table 1 in the main text. 'n =' refers to the number of samples for which the water content at sampling was available. Data was unavailable for the BOPA trial. **Figure S19:** Comparison of three mixed-effect models to estimate field penetration resistance (FPR). The model with the reduced dataset ($n = 76$) showed a poorer model fit compared to the original model. However, if the model selection procedure included saturation at the time of sampling as an additional variable, the model fit increased significantly. The 'Original model' refers to the full final model shown in Table 3. The 'Original model (without BOPA)' refers to a model that was selected and fitted to a reduced dataset where the BOPA site was omitted. The 'New model' refers to a model that was selected and fitted to the reduced dataset but included Saturation at the time of sampling as an additional variable in the initial model (before model selection). Saturation was calculated as the proportion of air filled soil pores at permanent wilting point, i.e., the ratio of the volumetric water content at sampling minus the volumetric water content at permanent wilting point to porosity minus the volumetric water content at permanent wilting point. 'R^2_m' and 'R^2_c' refer to the marginal and the conditional explained variance of the models, respectively. 'n =' refers to the number of observations in the dataset. Colours indicate the paradigm of the effect—blue is a positive effect, red a negative effect. BD, bulk density; SOC, soil organic carbon; STIR, soil tillage intensity rating. **Figure S20:** Water stable aggregate index (WSA) of the topsoil. The colour indicates the mean annual temperature (MAT) at the site where the sample was taken. The blue regression line reaches 99% of the saturation value (i.e., 0.65) at 16.5 g kg^{-1} soil organic carbon (SOC). **Figure S21:** Parial effect plots of linear and nonlinear responses to management and pedo-climatic drivers. Yellow represents the prediction of the linear model presented in Table 3 and green represents the prediction of the nonlinear model presented in Table S6. AIC and R^2_m refer to Akaike Information Criterion and the marginal R^2 of the respective model. The shaded areas represent the 95% confidence interval of the prediction. The black lines at the bottom of the plots indicate the predictor values in the dataset. All other predictors than the one depicted on the x-axis were set to the median predictor value in the dataset and no-random effects were considered. **Table S1:** Results of the methodological effect tests for saturated conductivity (K_{sat}), matrix conductivity (K_{5hPa}), plant available water (PAW) and air capacity at −100 hPa matric potential (AC). **Table S2:** The variability of the data was assessed by attributing the sum of squares (SS) to the different levels (LTE (= site), treatment and residual) in the data for each variable. This was done by running a series of sequential ANOVAs. The results for the topsoil and the subsoil are shown separately. N = 92. **Table S3:** Mean and standard deviation in brackets of measured soil parameters per LTE, treatment and depth. Significant differences between the mean values per treatment of a parameter within an LTE and depth are indicated: *** p-value < 0.001, ** p-value < 0.01, *p-value < 0.05, ·p-value < 0.1. Letters a, b and c indicate significant difference between treatments. Significance was tested with a two-way ANOVA that accounted for treatment and block effects. Abbreviations for LTEs and treatments can be found in Table 1 of the main text. **Table S4:** Number of parameter estimates of the final mixed-effect models that changed significantly if an LTE was left out of the dataset. Abbreviations of LTEs are the same as in Table 1 in the main text. **Table S5:** The estimates that inversed due to the leaving out of an LTE from the dataset. Abbreviations of LTEs are the same as in Table 1 in the main text. **Table S6:** Model summaries of the nonlinear mixed-effect models.